



UNIVERSIDADE DE LISBOA

Faculdade De Medicina

VALIDATION AND FURTHER CHARACTERIZATION OF
PSEUDOMONAS AERUGINOSA GENES PUTATIVELY
INVOLVED IN MODULATING MULTIDRUG RESISTANCE

Sara Cristina Fragata Pereira

Advisor: PD Dr. rer. nat. Erwin Bohn

Co-Advisor: Prof. Dr. Mário Nuno Ramos d'Almeida Ramirez

Interim Document

Thesis for the achievement of Master's degree in

Clinical Microbiology and Emerging Infectious Diseases

Trabalho final especialmente elaborado para obtenção do grau de Mestre em

Microbiologia Clínica e Doenças Infecciosas Emergentes



UNIVERSIDADE DE LISBOA

Faculdade De Medicina

VALIDATION AND FURTHER CHARACTERIZATION OF
PSEUDOMONAS AERUGINOSA GENES PUTATIVELY
INVOLVED IN MODULATING MULTIDRUG RESISTANCE

Sara Cristina Fragata Pereira

Advisor: PD Dr. rer. nat. Erwin Bohn

Co-Advisor: Prof. Dr. Mário Nuno Ramos d'Almeida Ramirez

Interim Document

Thesis for the achievement of Master's degree in

Clinical Microbiology and Emerging Infectious Diseases

Trabalho final especialmente elaborado para obtenção do grau de Mestre em

Microbiologia Clínica e Doenças Infecciosas Emergentes

2022

Acknowledgments

I would like to begin by expressing my deepest gratitude to my advisor, PD Dr. rer. nat. Erwin Bohn, who made this thesis possible. Without his guidance, support, and patience, this achievement would have been impossible. Dr. Bohn, thank you for welcoming me to your lab and to your country, providing me with valuable feedback and advice, and teaching me so much. I am honoured to have had the opportunity to work under your supervision, and I hope this thesis makes you proud.

I am also grateful to my co-advisor, Prof. Dr. Mário Ramirez, for his inspiring mentorship since the beginning of my Master's degree. Prof. Ramirez's unwavering support and motivation throughout the ups and downs of this project were instrumental in its completion.

I wish to express my heartfelt thanks to all the members of the Bohn/Schuetz research group, especially Michael, Kristina, Elias, Karolin, and Fabian, whose help and feedback were instrumental to the success of this thesis. I also want to dedicate a special thank you to my colleagues Johanna, Noelle, and Kathrin, whose support and kindness I couldn't have done without. You have been an amazing team to work with, and I am grateful for everything you have done for me.

Finally, I would like to thank my parents, Elsa Fragata and Artur Pereira, for their unwavering support and encouragement throughout my academic journey. I am also extremely indebted to my goddaughter Joana Saraiva, whose tireless dedication and scientific expertise were essential to the completion of this thesis. Afi your emotional support meant the world to me, you are the most hard-working person I've ever met, a great inspiration, thank you so much. Thank you all for being such an important part of my life and for supporting me every step of the way.

Thank you!

FLUCTUAT NEC MERGITUR

ABSTRACT

Pseudomonas aeruginosa, a Gram-negative bacteria, is one of the most relevant nosocomial pathogens. Pa's multidrug resistance has recently increased substantially.

The genes *amgK*, *anmK*, *bepA*, *murU*, *mupP* and *ycgE2* were identified in the TraDIS screen described in Sonnabend *et al.*. To validate the identification of these genes and investigate their relevance in antibiotic resistance we generated Pa ID40 Δ *bepA*, Δ *murU*, Δ *mupP* and Δ *ycgE2*.

We investigated whether the deletion of *amgK*, *anmK*, *bepA*, *murU*, *mupP* and *ycgE2* affected growth by performing growth curves. No significant differences were observed. To understand how the genes modulate resistance, minimal inhibitory concentrations were assessed: a reduction of 1- to 3-fold was observed for most beta-lactams and fosfomycin in Δ *anmK*, Δ *amgK*, Δ *mupP*, Δ *murU* and Δ *bepA*; and 2-fold for polymyxin B in Δ *amgK* and Δ *bepA*, in comparison to ID40. To determine if the decreased MICs are due to alterations of efflux pumps activity, activity efflux assays were performed for all mutants, where no differences to the WT were observed. Since the genes lead to increased beta-lactam resistance, beta-lactamase activity was assayed, and all mutants showed a decrease. To understand the gene's involvement in transcriptional regulation of AmpC, *ampC* expression was measured, being close (~ 1-fold) to the WT for all mutants. Because of the polymyxin B MIC reduction for Δ *amgK*, a serum killing assay was performed, and no differences between ID40 Δ *amgK* and WT were observed.

The studied genes don't affect bacterial fitness. *anmK*, *amgK*, *mupP*, *murU* and *bepA* modulate resistance by increasing beta-lactam and fosfomycin resistance and *amgK* and *bepA* by increasing polymyxin B resistance. Efflux/influx isn't involved in modulating resistance in the studied genes. All studied genes lead to increased beta-lactamase activity. How *anmK*, *amgK*, *mupP*, *murU* and *bepA* are involved in regulation of AmpC and the mechanism through which they modulate resistance remains unclear.

Key-words: *Pseudomonas*; Antimicrobial; Resistance; Peptidoglycan; Beta-lactamase

RESUMO

Pseudomonas aeruginosa (Pa) é uma bactéria Gram-negativa, anaeróbica facultativa, que é ubíqua no ambiente e capaz de causar doenças não só em seres humanos, mas também em animais e plantas. Pa é uma das espécies patogênicas nosocomiais mais relevantes, com a importância crescente das infecções causadas por estirpes multirresistentes. Esta espécie apresenta resistência a uma variedade de antibióticos, tais como antibióticos beta-lactâmicos, aminoglicosídeos e quinolonas, sendo que a resistência a múltiplos agentes antimicrobianos tem vindo a aumentar substancialmente nos últimos anos.

Os genes *amgK*, *anmK*, *bepA*, *murU*, *mupP* e *ycgE2* foram identificados através da análise de TraDIS descrita em Sonnabend *et al.* (2020). A identificação destes genes foi feita numa estirpe isolada em contexto clínico, a partir da corrente sanguínea, caracterizada como multirresistente, e denominada como Pa ID40 (estirpe *wild-type*, WT). (Willmann *et al.* 2019) Esta estirpe (Pa ID40) foi a utilizada ao longo deste trabalho, salvo indicação em contrário. A aplicação da técnica TraDIS permitiu a identificação de genes alvo (onde se incluem os genes em estudo nesta tese) com um possível envolvimento na capacidade desta estirpe resistir aos antimicrobianos. Os genes *amgK*, *anmK*, *mupP* e *murU* estão envolvidos na via de reciclagem de peptidoglicano. Esta via que reutiliza uma grande parte dos fragmentos resultantes da degradação da camada de peptidoglicano, constitui um novo alvo importante para terapêuticas antimicrobianas. (Dhar *et al.* 2018) O gene *bepA*, codifica a proteína BepA, uma zinco-metalopeptidase periplasmática, envolvida na manutenção da integridade da membrana externa e transporte de lipopolisacáridos. (Akiyama *et al.* 2021) Tendo isto em consideração, e de modo a validar a identificação dos genes encontrados pela análise do TraDIS, bem como determinar a sua relevância e potencial papel na resistência a diversos antimicrobianos, procedeu-se à geração de mutantes de deleção Pa ID40 Δ *bepA*, Δ *murU*, Δ *mupP* e Δ *ycgE2*. Para gerar os mutantes de deleção, em primeiro lugar, foi aplicada a clonagem de Gibson com recurso ao plasmídeo pexG2 e digestão com DpnI. Em seguida, foram realizadas transformações primeiro em TOP10 *E. coli* e depois em SM10 λ pir *E. coli*. Por fim, foi realizada a conjugação em Pa ID40 seguida de contra-seleção, e vários PCRs foram

feitos para validar o processo de mutação. É relevante, no entanto, referir que a geração dos mutantes Pa ID40 $\Delta anmK$ e $\Delta amgK$ foi realizada independente deste estudo.

De forma a atingir o objetivo definido, a caracterização dos mutantes de deleção é fundamental. Assim, a importância dos genes *amgK*, *anmK*, *bepA*, *murU*, *mupP* e *ycgE2* no padrão de crescimento foi determinada através da realização de curvas de crescimento em LB e em meio mínimo M9, durante um período de 36 horas. A análise destes resultados demonstrou a ausência de diferenças significativas entre as estirpes com mutação e a estirpe Pa ID40 WT. De forma a investigar a forma como os genes em causa modulam a resistência em Pa, foram estabelecidas as concentrações inibitórias mínimas (MICs) para um conjunto de diferentes antimicrobianos, nomeadamente beta-lactâmicos, fosfomicina e polimixina B. Para tal foram utilizadas as placas disponíveis comercialmente, “GN2F” e “EUX2NF” da Thermofisher, e “MICRONAUTS β -Lactamases” da Merlin. Os resultados mostraram uma redução de MIC para entre metade a um terço para a maioria dos beta-lactâmicos nas estirpes ID40 $\Delta anmK$, $\Delta amgK$, $\Delta mupP$, $\Delta murU$ e $\Delta bepA$ em comparação com a estirpe WT. Do mesmo modo, resultados idênticos foram observados para a fosfomicina. Por outro lado, ao analisar os resultados das MICs da polimixina B pudemos observar uma redução de MIC para metade nas estirpes ID40 $\Delta amgK$ e $\Delta bepA$, em comparação com a estirpe WT.

Efluxo é um processo utilizado por inúmeros organismos para diminuir a susceptibilidade a compostos tóxicos, tais como os antibióticos. Desta forma, para determinar se a diminuição de resistência observada nos mutantes, aquando da análise dos resultados da determinação das MICs, poderia ter origem em alterações na atividade das bombas de efluxo, a realização de ensaios de efluxo para todos os mutantes é fundamental, tendo sido por isso o próximo passo executado. Este ensaio teve como base o uso de um corante fluorescente, designadamente Hoechst 33342. Subsequentemente à sua entrada na célula, este corante cria uma ligação ao ADN de dupla cadeia, funcionando ao mesmo tempo como um substrato de várias bombas de efluxo. Assim, espera-se que o sinal luminescente detectado aquando da ligação de Hoechst 33342 reflita a proporção de influxo e efluxo. Os dados obtidos, no entanto, não revelaram quaisquer diferenças significativas entre os mutantes de deleção e a estirpe WT. Paralelamente, e uma vez que a deleção dos genes levou a uma diminuição da resistência a beta-lactâmicos, procedeu-se à medição da actividade da beta-lactamase. A atividade desta enzima foi medida recorrendo ao kit da companhia

BioVision com o nome de “ β -Lactamase Colorimetric Assay Kit”, que se baseia na quantificação de um produto da reação da hidrólise da nitrocefina, uma cefalosporina cromogénica. Estes ensaios, por sua vez, revelaram uma diminuição de 20 % a 70 % da actividade de beta-lactamase para todos os mutantes, quando comparados com a estirpe WT.

Posteriormente, a expressão de *ampC* foi determinada de modo a avaliar se a redução de actividade se deveria ao envolvimento dos genes em estudo na regulação transcricional da beta-lactamase AmpC, uma cefalosporinase cromossómica, com um papel major em conferir multirresistência em Pa. A análise da expressão de *ampC* foi, portanto, executada através de múltiplas reacções em cadeia da polimerase, quantitativas e em tempo real de transcrição reversa (qRT-PCR). Adicionalmente, a ausência de contaminação por ADN foi previamente estabelecida através da execução da reação em cadeia da polimerase quantitativa (qPCR), amplificando o gene conservado *gyrB*. Estes resultados mostraram que as estirpes mutantes têm um nível de expressão semelhante ao da estirpe WT, não sendo, por isso, mudanças de expressão a causa das alterações na actividade da beta-lactamase.

O sistema do complemento constitui a primeira linha de defesa imune, e é constituído por uma rede de proteínas plasmáticas que desencadeiam uma cascata proteolítica aquando do reconhecimento de certos padrões microbianos. Tendo isto em consideração, as bactérias são capazes de usar várias estratégias para obter resistência sérica. Uma vez que a estrutura do lipopolissacárido, relacionada com a resistência à polimixina B, é importante para alcançar a resistência sérica, especulou-se que a deleção de *amgK* poderia afetar a resistência sérica. Assim, o ensaio de morte sérica foi realizado, não tendo sido, no entanto, observadas diferenças entre o mutante de deleção *amgK* e a estirpe WT. Uma vez que a mesma diferença de MIC foi observada para *bepA* e para *amgK*, e considerando as funções de BepA, seria relevante realizar este ensaio com um mutante com deleção de *bepA*. Porém, devido a constrangimentos de tempo, não foi possível fazê-lo neste estudo.

No seu conjunto, estes resultados permitem a obtenção de diversas conclusões. Primeiramente, os genes estudados não afetam a capacidade de crescimento em condições normais de laboratório. Mais, os genes *anmK*, *amgK*, *mupP*, *murU* e *bepA* contribuem para a resistência a beta-lactâmicos e fosfomicina e os genes *amgK* e *bepA* contribuem para a resistência à polimixina B. Verifica-se então que os genes *amgK*, *anmK*, *mupP* e *murU*, todos eles genes envolvidos na via de reciclagem de peptidoglicano, modulam a resistência

antimicrobiana. Isto é indicativo da relevância da via de reciclagem do peptidoglicano na resistência antimicrobiana. Os resultados obtidos permitiram ainda concluir que o gene *bepA* também modula a resistência antimicrobiana, o que é pertinente visto que a proteína codificada por este gene tem um papel importante em manter a integridade da membrana externa assim como em transportar lipopolissacáridos para a mesma. Concluiu-se também que a modulação de resistência, observada na análise das MICs das estirpes com deleção dos genes em estudo, é independente da atividade de efluxo/influxo. Pelo contrário, concluiu-se que a modulação da resistência está relacionada com a atividade de beta-lactamase, que foi afectada em todos os genes estudados. No entanto, a expressão de *ampC* não parece ser afectada nas estirpes mutantes. Assim, a forma como os genes *anmK*, *amgK*, *mupP*, *murU* e *bepA* estão envolvidos na regulação da actividade da beta-lactamase e o mecanismo através do qual eles modulam a resistência não estão ainda esclarecidos.

Palavras-chave: *Pseudomonas*; Antimicrobiano; Resistência; Peptidoglicano; Beta-lactamase

Table of Contents

TABLE OF CONTENTS.....	XIII
TABLE OF FIGURES	XV
TABLE OF TABLES	XVI
TABLE OF ABBREVIATIONS.....	XVII
1. INTRODUCTION.....	1
1.1. <i>Pseudomonas aeruginosa</i>	1
1.2. Importance of <i>Pseudomonas aeruginosa</i>	3
1.3. Resistance mechanisms of <i>Pseudomonas aeruginosa</i>.....	4
1.4. Peptidoglycan recycling pathway in <i>Pseudomonas aeruginosa</i>	10
1.5. Research objectives	14
2. MATERIALS AND METHODS.....	15
2.1. Materials	15
2.1.1. Culture media	15
2.1.1.1. Lysogeny Broth medium (LB).....	15
2.1.1.2. LB agar medium	15
2.1.1.3. M9 minimal medium.....	15
2.1.1.4. Mueller Hinton Buillon medium	15
2.1.1.5. Super optimal broth with catabolite repression medium (SOC).....	15
2.1.2. Bacterial strains	16
2.1.3. Oligonucleotides	18
2.2. Methods	20
2.2.1. Generation of deletion mutants	20
2.2.2. Growth curves.....	25
2.2.3. Determination of Minimal Inhibitory Concentrations (MIC Assay)	27

2.2.4.	Efflux activity assay	28
2.2.5.	Beta-lactamase activity.....	29
2.2.6.	mRNA expression.....	30
2.2.6.1.	RNA isolation.....	30
2.2.6.2.	qPCR (quantitative Polymerase Chain Reaction)	32
2.2.6.3.	qRT-PCR (Reverse transcriptase Real-time PCR)	32
2.2.7.	Serum killing	33
3.	RESULTS AND DISCUSSION	36
3.1.	Generation of deletion mutants.....	36
3.2.	Growth curves	42
3.2.1.	Growth curves in LB medium.....	42
3.2.2.	Growth curves in M9 minimal medium	45
3.3.	Determination of Minimal Inhibitory Concentrations.....	48
3.4.	Efflux activity assay.....	53
3.5.	Beta-lactamase activity.....	55
3.6.	mRNA expression	58
3.7.	Serum killing.....	60
4.	CONCLUSION.....	65
5.	REFERENCES.....	67

Table of Figures

Figure 1 - Scanning electron micrograph of <i>Pseudomonas aeruginosa</i> bacilli.	1
Figure 2 - Lysogeny broth agar plate with colonies of ID40 strain of <i>Pseudomonas aeruginosa</i> demonstrating their blue-green colour.	2
Figure 3 - Transposon Directed Insertion Sequencing (TraDIS) procedure.	7
Figure 4 - Scheme of the peptidoglycan recycling and synthesis pathway of Pa adapted from Sonnabend <i>et al.</i>	13
Figure 5 - Representative image of the two-step allelic exchange procedure.	24
Figure 6 - Graphic representation of typical bacterial growth curve in culture medium.	25
Figure 7 - Overview of the Gibson Assembly Cloning Method.	37
Figure 8 - Identification of deletion mutants by PCR.	38
Figure 9 - Agarose gel 1 % electrophoresis of the colony-PCR products.	39
Figure 10 - Agarose gel 1 % electrophoresis of the colony-PCR products of the clones selected previously (Fig. 9).	41
Figure 11 - Growth curves of <i>P. aeruginosa</i> ID40 strain and mutants ($\Delta amgK$, $\Delta anmK$, $\Delta mupP$, $\Delta murU$, $\Delta bepA$, $\Delta ycgE2$) in LB medium.	43
Figure 12 - Growth curves of <i>P. aeruginosa</i> ID40 strain and mutants ($\Delta amgK$, $\Delta anmK$, $\Delta mupP$, $\Delta murU$, $\Delta bepA$, $\Delta ycgE2$) in M9 minimal medium.	46
Figure 13 - Efflux activity in ID40 and the deletion mutants ($\Delta amgK$, $\Delta anmK$, $\Delta mupP$, $\Delta murU$, $\Delta bepA$, $\Delta ycgE2$).	54
Figure 14 - β -Lactamase Activity Assay of ID40 WT and deletion mutants ($\Delta amgK$, $\Delta anmK$, $\Delta mupP$, $\Delta murU$, $\Delta bepA$, $\Delta ycgE2$).	56
Figure 15 - <i>ampC</i> expression in ID40 WT and deletion mutants ($\Delta amgK$, $\Delta anmK$, $\Delta mupP$, $\Delta murU$, $\Delta bepA$, $\Delta ycgE2$).	59
Figure 16 - Serum killing assay for assessment of optimal human serum concentration for ID40 WT strain.	61
Figure 17 - Serum killing assay of PA14 <i>P. aeruginosa</i> strains and the $\Delta amgK$ mutants.	62
Figure 18 - Serum killing assay of PAO1 <i>P. aeruginosa</i> strain and the $\Delta amgK$ mutants.	63

Table of tables

Table 1 - Susceptibility of ID40 WT and deletion mutants against different antibiotics.	8
Table 2 - Meropenem and cefepime resistome in Pa ID40.	9
Table 3 - Bacterial strains used.....	16
Table 4 - Deletion mutants generated.....	17
Table 5 - Plasmids used in this study.....	17
Table 6 - Primers for Gibson cloning.....	18
Table 7 - Flanking primers for confirmation of the deletion.....	19
Table 8 - qRT-PCR primers.....	19
Table 9 - Components and their respective quantities in μL for the performance of the KAPA HiFi PCR.....	21
Table 10 - PCR program used for the KAPA HiFi PCR.....	21
Table 11 - Components and their respective quantities in μL for the performance of the MangoMix PCR.....	22
Table 12 - PCR program used for the MangoMix PCR.....	22
Table 13 - Calculated size of PCR products, in base pairs (bp), according to the primers used in the PCR.....	39
Table 14 - Susceptibility of ID40 WT and deletion mutants against a variety of β -lactam, polypeptide and phosphonic antibiotics.	49
Table 15 - CP value results from qPCRs, with and without the presence of reverse transcriptase.....	58

Table of Abbreviations

ATP	- Adenosine 5'-triphosphate
BAM	- β -barrel assembly machinery
Bp	- Base pairs
CAP	- Community acquired pneumonia
cDNA	- Complementary deoxyribonucleic acid
CP	- Crossing Point
DNA	- Deoxyribonucleic acid
<i>E. coli</i>	- <i>Escherichia coli</i>
GC	- Growth curve
GlcNAc	- N-acetylglucosamine
Gm	- Gentamicin
HIS	- Heat inactivated human serum
LB	- Lysogeny broth
LPS	- Lipopolysaccharide
MDR	- Multidrug-resistant
MHB	- Mueller Hinton Buillon
MIC	- Minimal inhibitory concentration
mRNA	- Messenger ribonucleic acid
MurNAc	- N-acetylmuramic acid
n.a.	- Not available
NHS	- Normal human serum
OD	- Optical density
OM	- Outer membrane
<i>Pa</i>	- <i>Pseudomonas aeruginosa</i>
PBS	- Phosphate-buffered saline
PCR	- Polymerase chain reaction
PG	- Peptidoglycan
RLU	- Relative light units

RNA - Ribonucleic acid

RND - Resistance-nodulation-division

Rpm - Revolutions per minute

SOC - Super optimal broth with catabolite repression

Tn - Transposon

TraDIS - Transposon-directed insertion sequencing

UDP- GlcNAc - Uridine diphosphate N-acetylglucosamine

UDP-MurNAc - Uridine diphosphate N-acetylmuramic acid

WT - Wildtype

1. Introduction

1.1. *Pseudomonas aeruginosa*

Pseudomonas aeruginosa (Pa) is a Gram-negative, facultative anaerobic, asporogenous, rod-shaped, monoflagellated bacterium (Figure 1), ubiquitously occurring in the environment being capable of surviving under diverse environmental conditions. (1–3)

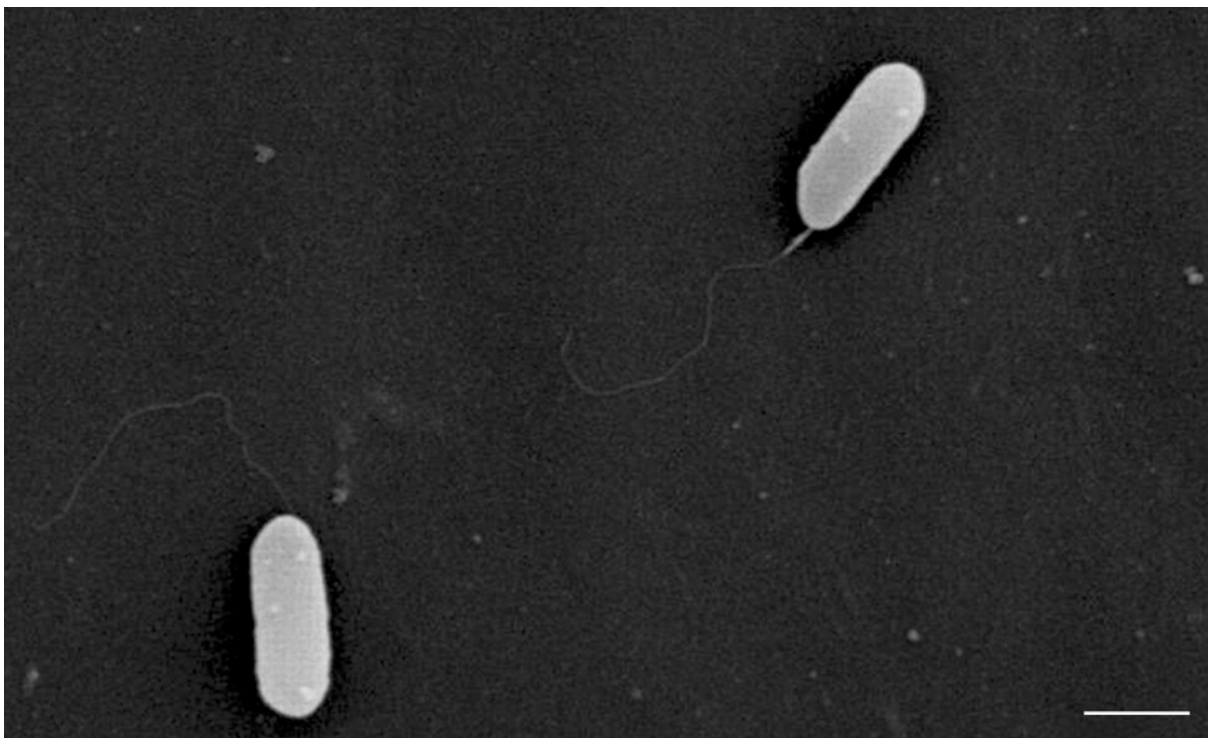


Figure 1 - Scanning electron micrograph of *Pseudomonas aeruginosa* bacilli.

Scale bar = 1 μm (3)

It causes disease in humans but also in plants and animals and it's responsible for serious infections in immunocompromised patients. (2) Like many other species, between the temperatures of 25°C and 37°C Pa grows easily but what distinguishes it from other *Pseudomonas* species is its ability to grow at temperatures as high as 42°C. (2) The characteristic smell of their colonies, although described differently by many people, may be said to be grape-like. (2) The colonies' colour, like their smell, is also a distinguishing

characteristic. Pa produces, amongst other pigments, pyocyanin, the most relevant pigment, which confers Pa its striking blue-green colour, observable in Figure 2. The name “*aeruginosa*” derives from the Latin word for copper rust which is the same hue as the pigment produced. Previous research has also revealed that pyocyanin contributes to the persistence of Pa in the lungs of cystic fibrosis patients as well as interferes with many cell functions, although the precise mechanism is yet unknown. (4)

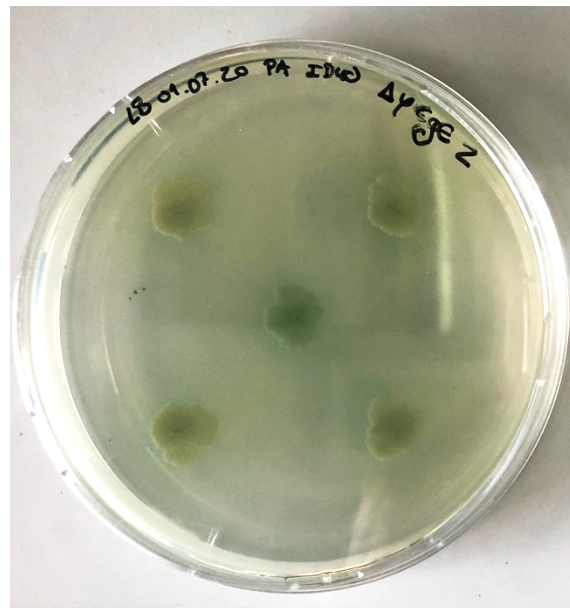


Figure 2 - Lysogeny broth agar plate with colonies of ID40 strain of *Pseudomonas aeruginosa* demonstrating their blue-green colour.

Pa’s genome consists of a single circular chromosome and is relatively large (5.5 - 7 Mbp) when compared to other Gram-negative bacteria, like *Escherichia coli* (*E. coli*) (4.6 Mbp). (2,5) The large genome allows for Pa to encode numerous enzymes and metabolic pathways allowing for its high nutritional versatility as well as carry many antibiotic resistance determinants conferring resistance to most antibiotic classes. (6) Moreover, around 8% of this large genome comprises regulatory genes, enabling Pa to adapt to complex growth environments. (2)

The outer membrane (OM) of the cell wall is an essential organelle of all Gram-negative bacteria. (2,7) The lipopolysaccharide (LPS) of Pa is less toxic when compared to the LPS of other Gram-negative bacteria. This constitutes an advantage, facilitating Pa’s establishment of chronic infections by inciting a low inflammatory response. (2)

Pa encodes multiple virulence factors, possessing a complex regulatory network for the expression of said factors. (2) Virulence factors include molecules, proteins and structures which help the bacterium colonize its host, they can be secreted, membrane associated or cytosolic. (8) Pa is able to express various virulence factors such as adhesins, secreted toxins and exoenzymes, and toxins directly injected into the host cell, as well as undergo a mucoid conversion through alginate overproduction, biofilm formation, and the most relevant for this research, antibiotic resistance. (2)

1.2. Importance of *Pseudomonas aeruginosa*

Treatment for Gram-negative caused infections has become one of the greatest challenges for physicians due to increasing antimicrobial resistance. (5,9) Pa is one of the most relevant nosocomial pathogens being particularly critical in intensive care units and immunocompromised patients. (9,10)

An increasing prevalence of nosocomial infections caused by multidrug-resistant (MDR) Pa strains has been observed and severely restricts treatment options leading to significant morbidity and mortality. (1,9) In recent years multidrug resistance has substantially increased. (9) Therefore carbapenem-resistant Pa was rated “priority 1: critical” of the World’s Health Organization list of priority pathogens for research and development of new antibiotics, demonstrating how important research on Pa resistance is. (11,12) In fact, Pa is so relevant in the medical context that the US Center for Disease Control and Prevention listed it as a pathogen of serious threat (level 2) and it is also one of the six highly virulent and antibiotic resistant bacterial pathogens which constitute the acronym “ESKAPE”. (13)

It has been shown that many risk factors linked to a higher infection severity (such as a higher Apache II score, the presence of underlying diseases, and intubation) as well as increased mortality are associated to the presence of resistant isolates. (9)

Pa is a leading cause of morbidity and mortality in cystic fibrosis patients. (2) It is also a leading cause of ventilator associated pneumonia and a rare cause of community acquired pneumonia (CAP), up to 8% of patients with CAP requiring intensive-care, but considered to have the highest mortality rate (>50 %). (9)

Pa also causes bloodstream infections, being the third leading cause of bacteremia amongst Gram-negative bacteria and being shown to lead to increased mortality in comparison to other Gram-negative infections as well as those caused by *Staphylococcus aureus*. (9)

Mortality rates are also shown to be higher (up to 20 %) in patients with Pa urinary tract infection. (9)

Pa is also particularly relevant in skin and soft tissue infections causing a variety of presentations and being one of the most commonly isolated pathogens from cellulitis in neutropenic patients, surgical site infections, infections resulting from trauma and infections of chronic decubitus ulcers. (9) The superficial wounds infected with Pa are characteristically yellow or green in colour and are also characteristically malodorous, in case of evolution of the infection to an invasive disease, a blue-purple lesion is frequently observable. (9) Among these variety of skin and soft tissue infections there are two clinical syndromes that are particularly important to refer: ecthyma gangrenosum and burn wound infection. (9) Ecthyma gangrenosum, a cutaneous vasculitis, is frequently reported in neutropenic patients with bloodstream infection. (9) In patients with burn wound infections, Pa is one of the most common causes, with a rate as high as 57 % of positive swabs or tissue culture, and a bloodstream infection rate in these patients of approximately 15 %. (9)

The overuse of antibiotics during treatment leads to an accelerated development of MDR Pa strains which contributes to the lack of efficiency of empirical antibiotic therapy. (5) This makes treatment much more difficult, resulting in an increasing number of intensive care unit admissions and deaths. (1) In order to undertake this issue, it is essential to further understand the resistance mechanisms of Pa and how to bypass them.

1.3. Resistance mechanisms of *Pseudomonas aeruginosa*

Pa exhibits resistance to a variety of antibiotics such as aminoglycosides, quinolones and β -lactams. To counter antibiotic attack, Pa possesses several mechanisms that can be divided into three types: intrinsic, acquired and adaptive resistance. (14)

In the intrinsic type it's worth noticing the extremely restricted outer membrane permeability of Pa, its highly developed efflux pump systems with particular focus on the

resistance-nodulation-division (RND) pumps which play a key role in antibiotic resistance. Also important is the production of antibiotic-inactivating enzymes, such as extended spectrum β -lactamases and amino-glycoside-modifying enzymes. (5,14)

When it comes to acquired resistance, it can be due to: mutations, responsible for modification of antibiotic targets, reduced antibiotic uptake, overexpression of efflux pumps and antibiotic-inactivating enzymes. (9) This is frequently mediated through the acquisition of resistance genes, which can be carried in plasmids, transposons, integrons and prophages, moreover bacteria can acquire these genes via horizontal gene transfer from the same or different bacterial species. (14)

The last class, adaptive resistance, increases the capacity of bacteria to survive in the presence of antibiotic molecules through temporary changes in gene and protein expression as a response to an environmental stimulus, being reversible once the stimulus is eliminated, biofilm-mediated resistance and the existence of a sub-population of persister cells are of the utmost importance for this class of resistance. (14)

Accumulation of various resistance mechanisms affecting different antimicrobials result in the emergence of MDR strains. Recent studies indicate that particularly the overexpression of AmpC, a chromosomal cephalosporinase, and components of efflux pumps play a critical role in conferring MDR. (1) *P. aeruginosa*, as many Gram-negative bacteria, has an inducible *ampC* gene that encodes the hydrolytic enzyme β -lactamase. This enzyme is able to break the amide bond of β -lactam ring, resulting in β -lactam antibiotics inactivation. (5)

Besides the presence of well characterized resistance genes which can be referred to as primary resistance genes (e.g. *ampC*), it has been recently demonstrated that additional chromosomally encoded non-essential genes may become essential in the presence of therapeutic concentrations of antibiotics.

In this thesis we looked specifically into susceptibility changes against three classes of antimicrobial drugs: β -lactams, polypeptide and phosphonic antimicrobials.

In the β -lactams class we specifically investigated monobactams, cephalosporins, carbapenems and ureidopenicillins. The β -lactams used include penicillin, cephalosporin, carbapenem and monobactam, which contain a β -lactam ring in their molecular structure. This class of antibiotics block bacterial cell wall biosynthesis by targeting the penicillin-binding proteins (PBPs), which are enzymes involved in peptidoglycan synthesis. (5)

Polymyxin belongs to the polypeptide class of antibiotics. These drugs are known to bind the lipopolysaccharides (LPS) on the outer membrane of Gram-negative bacteria, resulting in increased cell membrane permeability and antibiotic uptake. (5) Polymyxin B, in particular, is a polymyxin that is used in clinical practice, and leads to bacterial death through the induction of a hydroxyl radical mediated cell death pathway. (5) Importantly, to enter the bacterial cell, while β -lactams penetrate cell membranes through porin channels, polymyxins promote their own uptake by interacting with the LPS on the outer membrane of Gram-negative bacteria. (5)

Lastly, fosfomycin belongs to the phosphonic antibiotic class, being an epoxide derivative of phosphonic acid. Fosfomycin interferes with the first cytoplasmatic step of the bacterial cell wall biosynthesis - the formation of the peptidoglycan precursor uridine diphosphate N-acetylmuramic acid (UDP-MurNAc), resulting in decelerated peptidoglycan synthesis, reduced growth, and eventually cell lysis. (15) Because of its small size (138 Da) and polarity, fosfomycin can readily cross the outer membrane of Gram-negative bacteria through porins and in the *Pseudomonas sp.*, it is also actively transported into the cell by the glycerol-3-phosphate transporter GlpT. (15)

To search for genes contributing to resistance, Dr. Bohn's team used the multidrug-resistant clinical bloodstream isolate Pa ID40 (wild-type (WT) strain, resistant to carbapenems, cephalosporins and penicillins; see Table 1) to generate a transposon (Tn) library and used the Transposon-directed insertion sequencing (TraDIS) (16,17) for the identification of genes that become essential when bacteria are exposed to cefepime or meropenem at concentrations near the minimal inhibitory concentration (MIC). (Figure 3) Transposon insertion sequencing is a high-throughput technique for assaying large libraries of isogenic transposon mutants, providing information on genes' essentiality, function, and genetic interactions. This provides important information about the way this genetic variation can affect the bacteria's fitness. (16,17)

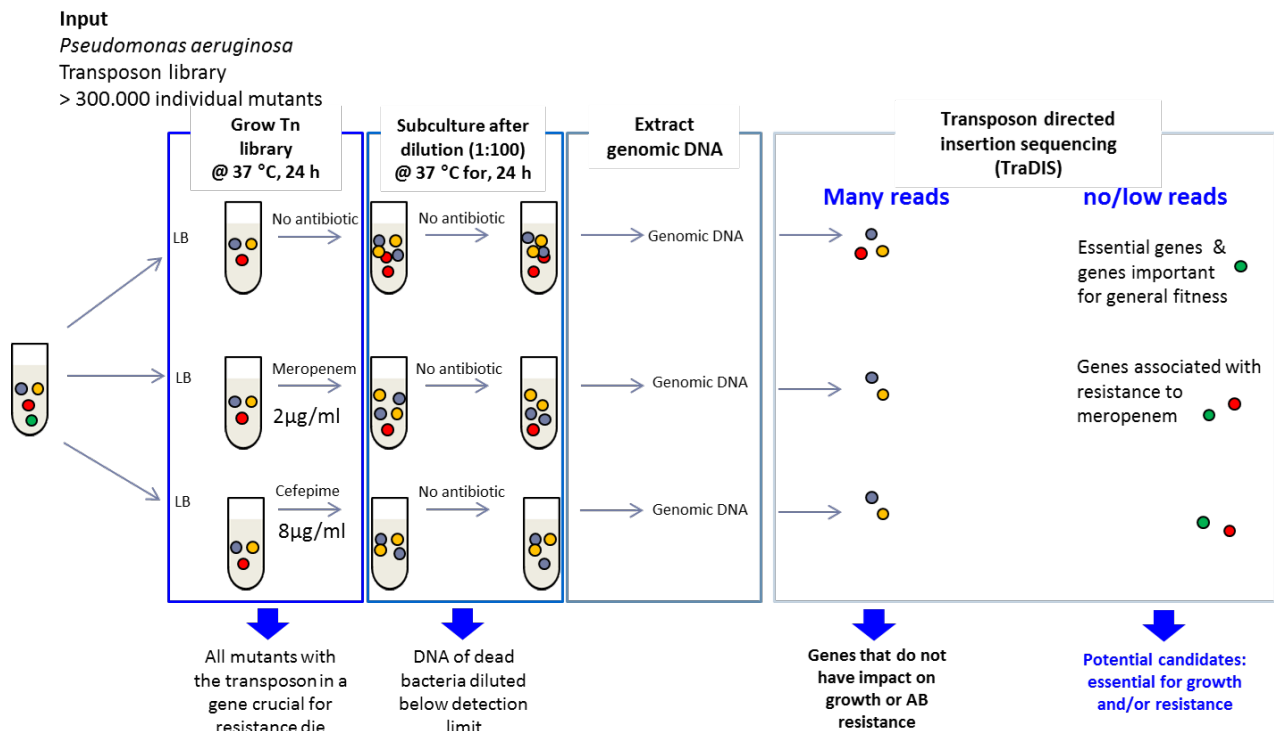


Figure 3 - Transposon Directed Insertion Sequencing (TraDIS) procedure.

Bacterial mutants with transposons in crucial genes for resistance are grown in LB at 37°C for 24 hours. Subculture is followed at the same conditions, in order to dilute the DNA of dead bacteria below the detection limit. The next steps include the extraction of genomic DNA, as well as the specific PCR amplification of the transposon-containing fragments. Lastly, a sequencing step will be performed, allowing the determination of key genes for growth and/or resistance. Each of the steps referenced are represented inside a rectangle. The circles in blue, red, yellow, and green stand for different genes. Image from Bohn *et al.*, unpublished.

Research revealed a common resistome for cefepime and meropenem which consisted primarily of genes involved in peptidoglycan synthesis or recycling, LPS biosynthesis, as well as several genes of unknown function (Table 2). Inhibition of such genes in combination with therapeutically used antibiotics may offer a novel strategy to treat Pa infections. The validity of the TraDIS approach has already been proven by deletion of three genes. In all cases deletion of the genes reduces resistance to cefepime, meropenem as well as piperacillin, as shown here for several deletion mutants. (10)

Table 1 - Susceptibility of ID40 WT and deletion mutants against different antibiotics.

Adapted from Sonnabend *et al.* (10)

(MEM, meropenem; IMP, imipenem; FEP, cefepime; CAZ, ceftazidime; PIP, piperacillin; PIT, piperacillin/tazobactam; ATM, aztreonam; FOS, fosfomycin)

	MIC Breakpoint [mg/L]		ID40 WT	$\Delta mltG$	$\Delta mepM1$	$\Delta ygfB$	$\Delta amgK$
	S \leq	R $>$					
MEM	2	8	8	2	4	4	4
IMP	4	4	>8	2	>8	8	8
FEP	8	8	>8	4	8	8	8
CAZ	8	8	>32	2	16	16	16
PIP	16	16	>32	<4	32	16	16
PIT	16	16	64	2	32	16	16
ATM	1	16	16	4	8	8	4
FOS	-	-	>64	64	64	>64	32

Minimal inhibitory concentrations (MIC) of ID40 WT and deletion mutant strains were determined by microbroth dilution. MIC values of the deletion mutants lower than that of ID40 WT are highlighted in green and those equal or below the MIC defining *in vitro* susceptibility are indicated in bold green. (10)

Table 2 - Meropenem and cefepime resistance in Pa ID40.

Adapted from Sonnabend *et al.* (10) In grey are the relevant genes for this thesis.

Category	Gene	Name/Function	MEM vs LB		FEP vs LB	
			Ratio	p value	Ratio	p value
Genes with an adjusted p value < 0.05 and ≥ 5-fold reduction for MEM and FEP						
Resistance	<i>ampC</i>	β-lactamase	0.07	0.00052	0.05	3.87·10 ⁻⁵
PG synthesis/ recycling	<i>mltG</i>	Endolytic murein transglycosylase	0.02	1.32·10 ⁻³³	0.03	1.77·10 ⁻⁴¹
	<i>mepM1</i>	Murein-DD endopeptidase	0.05	1.01·10 ⁻⁰⁷	0.07	2.29·10 ⁻⁰⁶
	<i>ftsW</i>	Synthesis of septal peptidoglycan during cell division	0.11	2.76·10 ⁻⁰⁵	0.20	0.0019
	<i>nagZ</i>	β-N-acetyl-D-glucosaminidase	0.07	1.56·10 ⁻⁰⁵	0.04	6.23·10 ⁻⁰⁶
	<i>anmK</i>	Anhydro-N-acetylmuramic acid kinase	0.12	4.938·10 ⁻¹⁰	0.20	1.62·10 ⁻⁰⁶
	<i>amgK</i>	N-acetylmuramate/ N-acetylglucosamine kinase	0.08	3.05·10 ⁻⁰⁶	0.17	0.0085
	<i>hddC/ murU</i>	Similar to N-acetylmuramate alpha-1-phosphate uridylyl-transferase murU of <i>Pseudomonas putida</i>	0.07	5.10·10 ⁻⁰⁵	0.15	0.0001
LPS	<i>wbpE</i>	UDP-2-acetamido-2-deoxy-3-oxo-D-glucuronate aminotransferase	0.10	1.58·10 ⁻⁰³	0.135	6.43·10 ⁻⁰³
Unknown	<i>ygfB</i>	ygfB-like proteins, unknown	0.06	2.35·10 ⁻¹⁹	0.06	5.56·10 ⁻²⁰
Genes with an adjusted p value < 0.05 and ≥ 5-fold reduction only for MEM						
PG synthesis/ recycling	<i>mepM2</i>	Murein DD-endopeptidase MepM, unknown function	0.14	3.60·10 ⁻¹²	0.37	0.002
β-barrel assembly	<i>bepA/ ygfC_1</i>	β-barrel assembly enhancing protease	0.12	2.17·10 ⁻⁰⁷	0.24	1.20·10 ⁻⁰⁶

Genes with an adjusted p value < 0.05 and ≥ 5-fold reduction only for FEP						
PG synthesis/ recycling	<i>gph_2/ mupP</i>	N-Acetylmuramic Acid 6-Phosphate Phosphatase MupP	0.27	0.14	0.185	$4.12 \cdot 10^{-02}$
	<i>mrcA</i>	Penicillin binding protein 1	0.73	0.40	0.05	$3.15 \cdot 10^{-12}$
	<i>lpoA</i>	Penicillin binding protein activator	1.03	1	0.20	$6.87 \cdot 10^{-16}$
Porin	<i>oprF</i>	Outer membrane protein F	0,22	0.036	0.20	0.03
Genes with an adjusted p value < 0.05 and < 5-fold reduction for MEM and FEP						
Unknown	<i>ycgE_2</i>	HTH-type transcriptional repressor YcgE	0.219	$1.32 \cdot 10^{-04}$	0.229	$1.93 \cdot 10^{-04}$

1.4. Peptidoglycan recycling pathway in *Pseudomonas aeruginosa*

Bacterial cells are encased and stabilized by a cell wall constituted of peptidoglycan (PG), a cross-linked polymer. (6,13,18,19) The PG cell wall is essential for the bacterial cells since it sustains the turgor pressure and stabilizes both the plasma and the outer membranes. (6,13,18,19) The PG layer, located in the periplasm, experiences constant renovation during bacterial growth. A large fraction of the PG turnover fragments that result from the PG layer degradation are often salvaged and reused via a pathway referred to as PG recycling. (6,18)

The greater part of cell wall recycling knowledge comes from the study of *Escherichia coli*, which turns over about 40 % of the PG layer per generation. (6,13,18,19)

The PG recycling pathway constitutes an important novel drug target for antimicrobial therapy since it's highly conserved and exclusive of bacteria. (6,18) Its association with beta-lactam antibiotic resistance, host innate immune response and bacterial differentiation and survival further reinforces its relevance as a drug target. The fact that the cell wall biogenesis pathway is already a target for several antibiotics such as penicillin and other beta-lactam drugs also emphasizes its well-established importance. (6,18)

PG synthesis depends on penicillin-binding proteins, which are the targets of beta-lactam antibiotics. Pa is frequently resistant to beta-lactams due to AmpC, a chromosomally encoded

beta-lactamase, like several other Gram-negative bacteria that rely on inactivation of beta-lactams by beta-lactamases. (19) The *ampC* gene expression is rigidly regulated in Pa and its induction is linked to cell wall stress. (19)

Pa has two periplasmic amidases, AmpDh2 and AmpDh3, that have an essential function in cell wall recycling. (13) Both these enzymes process the peptide chain on the polymeric peptidoglycan layer and 1,6-anhydromuramyl peptides that originated from the activities of lytic transglycosylases (LTs). (13) The PG layer is the preferred substrate for both enzymes, but AmpDh3 shows a higher specific activity for it than AmpDh2. (13)

The PG layer is constituted by a cross link of two chains of alternating N-acetylmuramic acid (MurNAc) and N-acetylglucosamine (GlcNAc), which are linked between themselves by $\beta(1\rightarrow4)$ glycosidic bonds. The MurNAc has attached to it a pentapeptide side chain, normally consisting of L-alanine- γ -D-glutamate meso-diaminopimelic acid-D-alanyl-D-alanine (L-Ala- γ -DGlu-m-DAP-D-Ala-D-Ala).

De-novo peptidoglycan biosynthesis starts in the cytoplasm. Fructose-6-phosphate is converted in several steps by GlmS, GlmM and GlmU into uridine diphosphate N-acetylglucosamine (UDP-GlcNAc), which is then converted into uridine diphosphate N-acetylmuramic acid (UDP-MurNAc) by MurA and MurB, and further into UDP-MurNAc-pentapeptide by the addition of a peptide chain by ligases MurC, MurD, MurE and MurF. (Fig. 4) (10,19)

The PG recycling pathway is an alternative route to generate UDP-MurNAc-pentapeptide, which bypasses the *de-novo* biosynthesis pathway. This pathway begins with the transport into the cytoplasm of muropeptides (GlcNAc-1,6-anhMurNAc-peptides) and GlcNAc-anhMurNAc, by permeases AmpG and AmpP. After the import, recycling begins with NagZ degrading the muropeptides into GlcNAc and 1,6-anhMurNAc-peptides. The 1,6-anhMurNAc-peptides are then degraded by AmpD into tripeptides L-Ala-iso-D-glutamate-mDAP and AnmK's substrate, 1,6-anhMurNAc. Subsequently MurNAc-6P is generated by the phosphorylation of 1,6-anhMurNAc by AnmK, an anhydro-N-acetylmuramic acid kinase. The phosphatase MupP hydrolyzes MurNAc-6P to MurNAc which is then processed into MurNAc-1P by the sugar kinase AmgK. The uridylyltransferase MurU then converts MurNAc-1P to UDP-MurNAc and further into UDP-MurNAc-pentapeptide by the addition of a peptide chain by

ligases MurC, MurD, MurE and MurF, which is an equal step to the *de-novo* biosynthesis pathways' UDP-MurNAc to UDP-MurNAc-pentapeptide reaction.

In order to integrate the PG cross-polymer, UDP-MurNAc-pentapeptide is transformed into GlcNAc-MurNAc peptides in several steps by several enzymes. The integration is made by high molecular mass penicillin-binding proteins, glycosyltransferases (GTFs), transpeptidases (TPs) and DD-carboxypeptidases (CPs).

To cleave the existent PG layer, low molecular mass penicillin-binding proteins, endopeptidases (EPs), lytic transglycosylases (LTs) and amidases such as AmpDh2, are necessary. Cleaving facilitates the integration of new glycan strands as well as simultaneous release of the PG degradation products, from the matrix to the cytoplasm.

Under normal conditions, 1,6-anhydro-MurNAc-peptides bind to the regulator AmpR inducing *ampC* expression, while UDP-MurNAc-pentapeptides bind to AmpR repressing *ampC* expression. As so, the balance between 1,6-anhMurNAc-peptides and UDP-MurNAc-pentapeptides is extremely important for the expression level of *ampC*. Shifting this balance by loss of either AmpG or NagZ will result in a reduced amount of 1,6-anhMurNAc-peptides and consequently reduce resistance against β -lactam antibiotics. On the contrary, loss of AmpD causes accumulation of 1,6-anhMurNAc-peptides and hence an increased *ampC* expression, which is a common cause of high constitutive *ampC* expression in clinical strains. (10,19)

Upon the introduction of β -lactams, the PG-crosslinks are blocked, which increase the turnover of muropeptides, and consequently result in the accumulation of 1,6-anhMurNAc-pentapeptide in the cytoplasm. The 1,6-anhMurNAc-muropeptides are able to displace UDP-MurNAc-pentapeptides from AmpR, which results in the derepression and hence activation of *ampC* transcription. (10) After AmpC is produced and exported to the periplasm, the β -lactam molecules are disabled by hydrolysis, consequently homeostasis ensues, which leads to a decrease in cytoplasmic anhydro-muropeptide levels and therefore repression of *ampC*. (19)

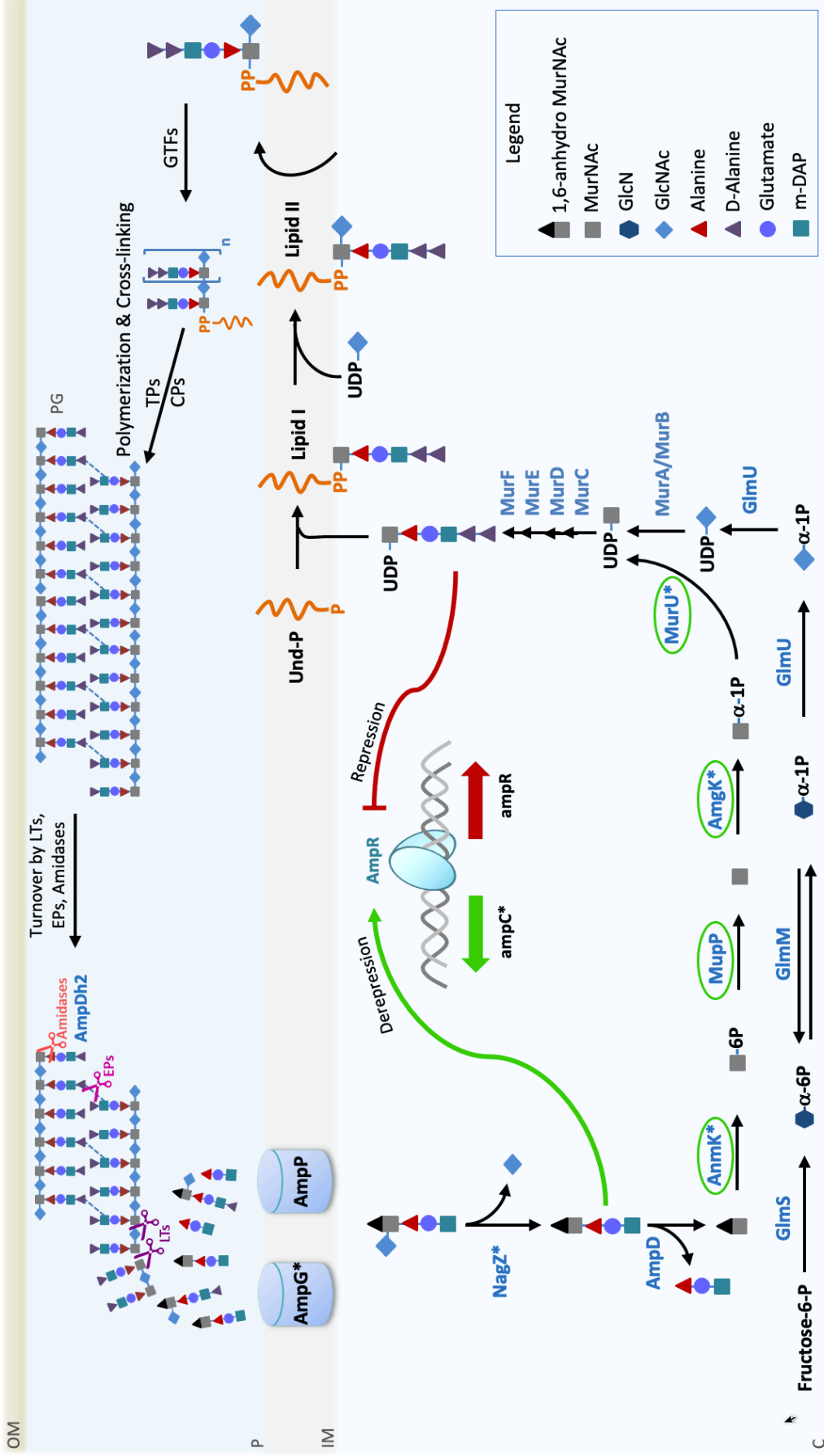


Figure 4 - Scheme of the peptidoglycan recycling and synthesis pathway of *Pa* adapted from Sonnabend *et al.*. The proteins studied in this thesis are highlighted in a green circle. An asterisk (*) is placed on the proteins mediating derepression of *ampC* expression. OM, outer membrane; P, periplasm; IM, inner membrane; C, cytoplasm; PG, peptidoglycan; CPS, peptidoglycan; GTFs, glycosyltransferases; EPs, endopeptidases; LTs, lytic transglycosylases. (10)

1.5. Research objectives

This thesis main objective is to understand whether additional genes identified in the TraDIS screen can also reduce resistance against β -lactam antibiotics, focusing predominantly on proteins forming the recently described salvage/recycling pathway including the products of the *anmK*, *mupP*, *murU* and *amgK* genes, which play a critical role in peptidoglycan recycling and intrinsic fosfomycin resistance. Deletion of *amgK* already indicated that this pathway contributes to antibiotic resistance. (10) It will be addressed whether all genes of this pathway are critical for antibiotic resistance and how these genes are involved in transcriptional regulation of the β -lactamase AmpC. In addition, it will be further tested whether two other genes, *bepA* and *ycgE2*, found in the TraDIS screening approach are involved in antibiotic resistance.

2. Materials and Methods

2.1. Materials

2.1.1. Culture media

2.1.1.1. Lysogeny Broth medium (LB)

The LB were prepared by mixing 10 g tryptone, 5 g yeast extract, 10 g NaCl, adjusting the pH to 7.5 using NaOH and adding 1 L of purified water. After prepared, the media were autoclaved.

2.1.1.2. LB agar medium

The LB agar were prepared by adding 15 g bacto agar to 1 L LB. After prepared, the media were autoclaved.

2.1.1.3. M9 minimal medium

The M9 media were prepared by adding 375 mL sterile Ampuwa water, 100 mL autoclaved 5x M9 minimal salts (Sigma-Aldrich, Cat. No: M6030), 1 mL 1 M filtered MgSO₄, 5 mL filtered 100x trace elements (from a stock solution with the following composition: EDTA 5 g /L; FeCl₃-6H₂O 0.83 g/L; ZnCl₂ 84 mg/L; CuCl₂-2H₂O 13 mg/L; CoCl₂-2H₂O 10 mg/L; H₃BO₃ 10 mg/L; MnCl₂-4H₂O 1.6 mg/L), 0.05 mL filtered 1M CaCl₂. 2.2 g of the carbon source, sodium pyruvate, were filtered, dissolved in 10 mL sterile Ampuwa water and then mixed with the other reagents. The volume was then made up to 500 mL with sterile Ampuwa water. All filtrations were performed using 0.22 µm sterile filters.

2.1.1.4. Mueller Hinton Bouillon medium

The Mueller Hinton Bouillon media used for this thesis' research were acquired from BioTrading Benelux B.V. with the designation of Mueller Hinton II Broth Micronaut.

2.1.1.5. Super optimal broth with catabolite repression medium (SOC)

The SOC media were prepared by mixing 20 g tryptone, 5 g yeast extract, 10 mL 1 M MgSO₄, 10 mL 1 M MgCl₂, 10 mL 1 M KCl, 2 mL 5 M NaCl, 20 mL 1 M Glucose and 1000 mL purified water.

2.1.2. Bacterial strains

Liquid cultures were grown at 37°C in a shaking incubator at 200 rpm (unless otherwise stated). Bacterial plates were incubated overnight at 37°C (unless otherwise stated). Bacterial strains used in this thesis are listed in Table 3.

Table 3 - Bacterial strains used

Bacterial strain	Reference number	Characteristics	Origin
Pa ID40	141	Multi-drug resistant clinical isolate	Willmann <i>et al.</i> 2019 (20)
Pa PA14 DSM-19882	1	Laboratory <i>Pseudomonas aeruginosa</i> strain	DSMZ (Nr. 19882)
Pa ID40 $\Delta amgK$	294	In-frame deletion of the <i>amgK</i> gene in the Pa ID40 background	Sonnabend (10)
Pa PAO1 DSM-19880	2	Laboratory <i>Pseudomonas aeruginosa</i> strain	DSMZ (Nr. 19880)
Pa PAO1 $\Delta amgK$	296	In-frame deletion of the <i>amgK</i> gene in the Pa O1 background	Mayer Group (15)
Pa ID40 $\Delta anmK$	297	In-frame deletion of the <i>anmK</i> gene in the Pa ID40 background	Bohn/Schütz Research Group
<i>E. coli</i> Top 10	Not applicable	Top-10 strain of <i>E. coli</i> with high efficiency of transformation	Thermo Fisher Scientific, Schwerte
<i>E. coli</i> SM10 λ pir	Not applicable	SM10 λ pir strain of <i>E. coli</i> with high efficiency of transformation	Hmelo <i>et al.</i> 2005 (21)

Table 4 - Deletion mutants generated

Name	Reference number	Characteristics
Pa ID40 Δ <i>bepA</i>	333	In-frame deletion of the <i>bepA</i> gene in the Pa ID40 genetic background
Pa ID40 Δ <i>murU</i>	345	In-frame deletion of <i>murU</i> gene in the Pa ID40 genetic background
Pa ID40 Δ <i>mupP</i>	337	In-frame deletion of <i>mupP</i> gene in the Pa ID40 genetic background
Pa ID40 Δ <i>ycgE2</i>	341	In-frame deletion of Δ <i>YcgE2</i> gene in the Pa ID40 genetic background
Pa PA14 Δ <i>amgK</i>	316	In-frame deletion of Δ <i>amgK</i> gene in the Pa ID40 genetic background (made in collaboration with Dr. Erwin Bohn)

Table 5 - Plasmids used in this study

Plasmid Name	Characteristics	Origin
pEXG2	Cloning-vector with pBR origin of replication; Gm resistance cassette; <i>sacB</i> gene	Hmelo <i>et al.</i> (21)
pEXG2 Δ <i>bepA</i>	pEXG2 derivative for in-frame deletion of the <i>bepA</i> gene	This study
pEXG2 Δ <i>murU</i>	pEXG2 derivative for in-frame deletion of the <i>murU</i> gene	This study
pEXG2 Δ <i>mupP</i>	pEXG2 derivative for in-frame deletion of the <i>mupP</i> gene	This study
pEXG2 Δ <i>ycgE2</i>	pEXG2 derivative for in-frame deletion of the <i>ycgE2</i> gene	This study

E. coli Top 10 was used due to its maximized cloning efficiency and enhanced genomic DNA cloning capabilities, while *E. coli* SM10 λ pir was used as a mobilizing strain because it carries the transfer genes of a broad host range.

The plasmid used to generate the mutants was pEXG2 (GenBank: KM887143.1) (Table 5), a cloning-vector with a pBR origin of replication (which is non-functional in Pa), a gentamicin resistance cassette and the *sacB* gene, used for counterselection, Hmelo *et al.* (2015). (21)

2.1.3. Oligonucleotides

Table 6 - Primers for Gibson cloning

Name	Reference number	Sequence (5' - 3')
990 pEXG2_MurU_up_f	990	AGCTAATTCCACACATTATACGAGCCGGA AGTGCATGTGCCGAGGATTCTC
991pEXG2_MurU_up_r	991	GCGTGCTCCGCCAGCAATCGCTCGACTT CCTTGGGCGTGTGCAGGG
992pEXG2_MurU_dn_f	992	ATGCGGCCGACCACCCTGCACACGCCCAA GGAAGTCGAGCGATTGCTGG
993pEXG2_murU_dn_r	993	TCGAGCCCGGGGATCCTCTAGAGTCGACC TTCACGCTCTCGGACCAGG
997pEXG2_MupP_up_f	997	AGCTAATTCCACACATTATACGAGCCGGA ACATGAGGTACAGGTAGACCGGC
998pEXG2_MupP_up_r	998	ATGCGGCTCAAAGCGGTACTGTTTCGACAT GGAACTCATCGACGTTCTCGACC
999pEXG2_MupP_dn_f	999	GAGCGCGGGTTCGAGAACGTCGATGAGT TCCATGTGCAACAGTACCGCTTTG
1000pEXG2_mupP_dn_r	1000	CGAGCCCGGGGATCCTCTAGAGTCGACCT GCCAAAGCTGGCAACATGAAG
1011pEXG2_bepA_up_f	1011	AGCTAATTCCACACATTATACGAGCCGGA ACAGCAGGACCACCAGGAACAG
1012pEXG2_bepA_up_r	1012	TCAGCGGAACATTTCTTGACCATCTTTTC CGCGTCAACAGGGCAGGGCG
1038 bep down F new	1038	TGAATGTACTGCGCCCTGCCCTGTTGACG CGGAAAAGATGGTCAAGGAAATGTTT
1014pEXG2_bepA_dn_r	1014	TCGAGCCCGGGGATCCTCTAGAGTCGACC TTTCTCGGCATTCTGCGACC
1018pEXG2_YcgE2_up_f	1018	AGCTAATTCCACACATTATACGAGCCGGA AGTGCCTACATCCGGAATTG
1019pEXG2_YcgE2_up_r	1019	TCACTTCTTCAGGACCAGCAGGACTTCCTC CAGCTCGTCGTTATGACTTG
1020pEXG2_YcgE2_dn_f	1020	ATGCTGGAACCAAGTCATAACGACGAGCT GGAGGAAGTCCTGCTGGTCC

1021pEXG2_YcgE2_dn_r	1021	TCGAGCCCGGGGATCCTCTAGAGTCGACC TATTACAACGAACACCGACCG
899pEXG2_amgKupF	899	AGCTAATTCCACACATTATACGAGCCGGA ACACCAGCATGCCCTTGTCG
900pEXG2_amgKupR	900	GGGACGGCGCGCCACGGCGGTTTCCAGA TACAGCTGCTGAAACGGGC
901pEXG2_amgK down F	901	ATGTCTGATGATGCCCGTTTCCAGCAGCT GTATCTGAAACCGCCGTGGC
902pEXG2_amgK down R	902	TCGAGCCCGGGGATCCTCTAGAGTCGACC TAACCTGCGGTCCAGCAGTTG

Table 7 - Flanking primers for confirmation of the deletion

Name	Reference number	Sequence (5'- 3')
pEXG2_seq_f	3	TACTGTGTTAGCGGTCTG
pEXG2_seq_r	4	GATCCGGAACATAATGGTG
994MurU_seq_f	994	CGTATCTGTCACCGCGAC
995murU_seq_r	995	CTGCGGTCCAGCAGTTG
996 murU inside_r	996	GAGATAGGCCTCGATCTGCTC
1001MupP_seq_f	1001	CGGTCTTTCAGCAGGTCTG
1002mupP_seq_r	1002	ACGATTTCCGCAAGTTCATC
1003mupP inside_r	1003	GTTCCAGGGTGCTGGTCT
1015_bepA_seq_f	1015	CGGGTCTCGGGCAGATAC
1016_bepA_seq_r	1016	GAAATCTTCGTGACCCGG
1017_bepA inside_r	1017	TCGCGGATGAGGATGAAGG
1022_YcgE2_seq_f	1022	CCGCGTTGTCACCTTTC
1023_YcgE2_seq_r	1023	ACAAACGGTCACCAGATACAG
1024_YcgE2 inside_r	1024	TGAAGCCCTGGTCGTAGAG
903amgKproof1	903	TGTTAATCCGGGCTTCCTGCG
904amgKproof2	904	CCGGCGGGCAGGATCATC
905amgK proof3	905	CCTGCCAGCGGAAATAACGAC

Table 8 - qRT-PCR primers

Name	Reference number	Sequence (5'- 3')
PA14_gyrB_f	13	CGTAACCTGAACAACACTACATCGAG
PA14_gyrB_r	14	AAGTACTTGCCCATCTCCTGTTC
ID40_ampC neu_f	77	TGCTGCTCCATGAGTCGTTT
ID40_ampC neu_r	78	CGCCTCTATTCCAACCCGAG

2.2. Methods

All methods that carried a risk of media or sample contamination or where the procedure could expose the operator to the bacteria being handled were performed in a laminar flow chamber.

2.2.1. Generation of deletion mutants

The ability to genetically manipulate bacteria has become a fundamental tool in studying bacteria and, although basic cloning has become an ordinary task in many laboratories, generating directed mutations can be a daunting task. (22)

Deletion mutants are defined by the loss of a number of nucleotides, in this case a sequence corresponding to the entirety of the desired gene.

To generate the deletion mutants first, Gibson Cloning was applied, with resource to the pexG2 plasmid and DpnI digestion. Next, transformations firstly into TOP10 *E. coli* and then into SM10 λ pir *E. coli* were performed. Finally, conjugation into Pa ID40 and counter selection was carried out, and several PCRs were done to validate the mutation process. This set of general steps are described in further detail hereafter.

Bacteria were cultivated overnight at 37°C with shaking at 200 rpm on lysogeny broth medium (LB) containing suitable antibiotics if necessary. Antimicrobials were added at the following concentrations: irgasan (25 μ g/mL; Sigma Aldrich #72779), and gentamicin (Gm; AppliChem #A1492) 15 μ g/mL (*E. coli* strains) or 75 μ g/mL (Pa strains). In-frame deletion mutants were generated using the suicide plasmid pEXG2 (21)). The primers used for the generation of deletion mutants and deletion verification are listed in tables 6 and 7. In order to amplify the selected segments of the Pa ID40 genome, KAPA HiFi PCR Kits, were used, as described in tables 9 and 10. KAPA HiFi PCR are high-fidelity PCR kits and offer error rates 100 times lower than that of wild-type *Taq*, as well as higher success rates, yields and consistency than those achievable with wild-type B-family DNA polymerases, and doesn't require accessory proteins or DNA binding domains. The intrinsic high processivity of the enzyme

results in significant improvements in yield, sensitivity, speed, as well as the ability to amplify difficult (GC- and AT-rich) and long amplicons.

Table 9 - Components and their respective quantities in μL for the performance of the KAPA HiFi PCR

Component	Quantity (μL)
Kapa HiFi GC buffer	5
10 mM dNTP Mix	0.75
Kapa Polymerase	0.5
Forward Primer	0.75
Reverse Primer	0.75
Template gDNA ID40 (20 ng/ μL)	1
H ₂ O	16.25
Total	25

Table 10 - PCR program used for the KAPA HiFi PCR

Reaction	Temperature	Duration	
Initial Denaturation	95°C	5 min	25x
Denaturation	95°C	30 sec	
Annealing	52-65°C	30 sec	
Extension	72°C	30 sec per kb	
Final Extension	72°C	5 min	
Pause	4°C	∞	

First, the flanking regions (consisting of 30bp at the 3' end and 30bp at the 5' end of the gene of interest plus approximately 800 bp for each flanking region) were amplified by KAPA PCR, purified with the Promega Wizard SV Gel and PCR clean-up system and ligated through Gibson assembly, mixing 10 μL of Gibson mix, around 150 ng of the up fragment and 150 ng of the down fragment, with the linearized pEXG2 (about 150 ng in 0.5 μL). (23) Then the mix was incubated for 30 minutes at 50°C. Next, the sample was placed shortly on ice, and then digested with 1 μL of DpnI for at least 1 hour at 37°C.

For the generation of the *E. coli* TOP10 strain containing the pEXG2 plasmid with the aimed gene, the pEXG2 vector (now in the Gibson mix, 8 μL) is mixed with previously prepared competent cells (*E. coli* TOP 10, Thermo Fisher Scientific, Schwerte) and submitted to thermal shock (20 minutes on ice, 30 seconds on 42°C water bath, 2 minutes on ice). Subsequently, 1 mL of SOC medium was added, and the samples were incubated with shaking for 1 hour. This culture was then spin-downed at 4000 g for 3 minutes, the supernatant was removed, and

the bacteria resuspended in LB, being finally plated in LB with Gm 15 µg/mL and incubated overnight. From these plates, bacteria were inoculated in 20 mL LB with 30 µL Gm, in order to perform a transformation confirmation colony-PCR, using MangoMix PCR (tables 11 and 12). For Colony-PCRs, purified DNA is not used as template but simply a small amount of colony material, which was resuspended in distilled water and boiled for 5 minutes in a Thermomixer Comfort (Eppendorf). Afterwards, cell debris was removed by centrifugation (4500 rpm for 5 minutes) and the supernatant, that contains the bacterial DNA, used as template DNA for the Colony-PCR.

Table 11 - Components and their respective quantities in µL for the performance of the MangoMix PCR

Component	Quantity (µL)
MangoMix	7.5
Forward Primer	0.5
Reverse Primer	0.5
Template:	
Isolated gDNA (20-40 ng)	1
Supernatant of lysed colony material	3
H ₂ O	Adjust
Total	15

Table 12 - PCR program used for the MangoMix PCR

Reaction	Temperature	Duration
Initial Denaturation	95°C	5 min
Denaturation	95°C	30 sec
Annealing	52-72°C	30 sec
Extension	72°C	30 sec per kb
Final Extension	72°C	5 min
Pause	4°C	∞

After the insert confirmation through colony PCR, DNA was isolated and purified with the Monarch Plasmid Miniprep kit according to the manufacturer's instructions and the constructed plasmids were verified by DNA sequencing. If the sequence presented the construct of interest with no undesirable mutations, the DNA was then used for transformation of competent *E. coli* SM10 λ pir (prepared according to Hmelo *et al.* (2005), 1 µL DNA with 50 µL *E. coli* SM10 λ pir) which were subsequently subjected to thermal shock (20 minutes on ice, 30 seconds on 42°C water bath, 2 minutes on ice), 1 mL of SOC medium is

then added. Subsequently, the samples were incubated with shaking for 1 hour, followed by a spin-down at 4000 g for 3 minutes. The supernatant was then removed, the bacteria resuspended in LB and finally plated in LB with Gm 15 µg/mL and incubated overnight. Posteriorly, bacteria was scraped and grown in 6 mL LB with 9 µL Gm.

Once the desired DNA sequence is in *E. coli* SM10 λ pir, conjugation was used to transfer it to Pa ID40. During conjugation the genetic material is transferred from the donor bacterium to the recipient bacterium, once in direct contact. (24,25) Conjugation was achieved by combining 200 µL of the donor strain, *E. coli* SM10 λ pir and 400 µL of the recipient strain, ID40 Pa, in LB. Further, a spin down (10000 g for 1 minute) was carried out, the bacteria were resuspended in 100 µL of LB and were then spot plated in an LB plate.

Positive selection of bacteria, where the plasmid was integrated into the chromosome, was achieved by plating onto a medium containing gentamicin. The strain used to transfer the plasmid into Pa, *E. coli* SM10 λ pir, was killed by the addition of 25 µg/mL irgasan to the medium. Since Pa is resistant to irgasan, plates containing both irgasan and gentamicin only allow for the growth of recipient Pa strains. These strains were grown on LB without any selection supplementation. During this time a second crossover may occur in a fraction of the population. These second crossovers result either in the deletion of the chosen gene or in the return to the wildtype genotype. To select for bacteria in which the second crossover occurred, a sucrose counter selection is performed. The allelic exchange vector that was initially used contains the *sacB* gene derived from *Bacillus subtilis*, which encodes the enzyme levan-sucrase catalyzing the hydrolysis of sucrose and the generation of the toxic metabolite levan.

In *E. coli* and Pa, the expression of *sacB* in the presence of sucrose is lethal, thus growth on LB plates containing sucrose leads to an enrichment in bacteria in which the second crossover has happened and the *sacB* gene was lost accordingly. As a consequence, these bacteria will also lose the gentamicin resistance cassette. Knowing this, bacteria were grown in parallel on LB plates and on LB plates with gentamicin. Bacteria that do not grow on LB with gentamicin plates are those in which the second crossover happened. (Fig. 5) (21) The chance that the second crossover leads to a deletion of the targeted gene or to a reversion to the wildtype genotype is 1:1. Quite often fitness disadvantages resulting from the introduced

mutation reduce the probability of getting mutants. Therefore, a significant number of colonies were screened by PCR to identify those with the desired crossover event.

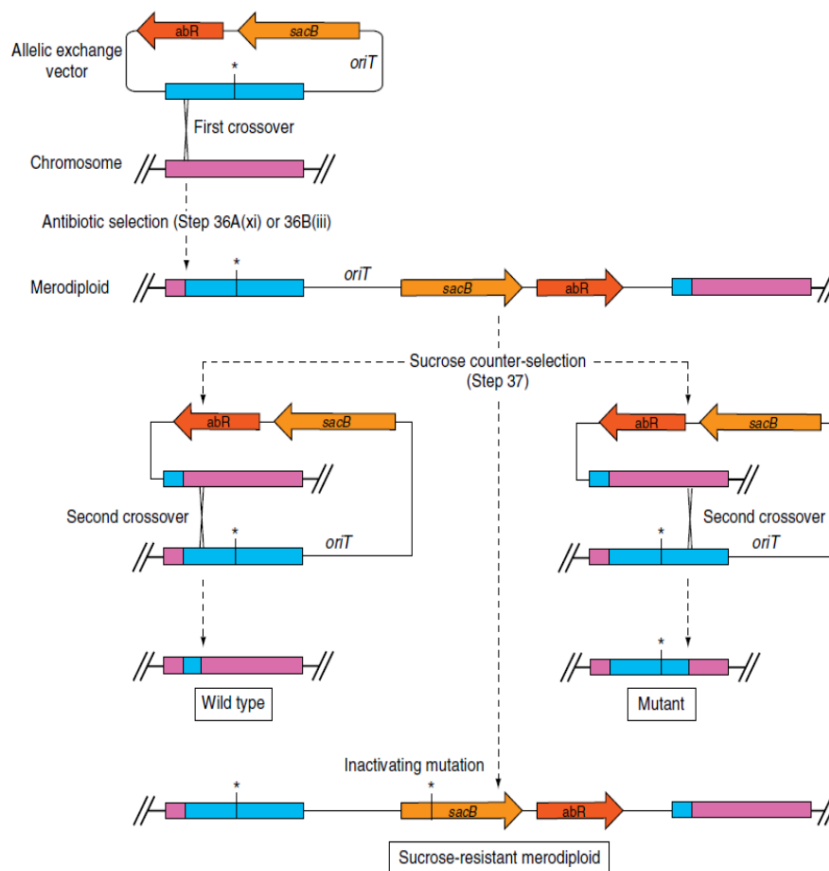


Figure 5 - Representative image of the two-step allelic exchange procedure.

Image from Hmelo *et al.* (21)

The bacteria which were spot plated, were incubated overnight at 37°C. The next day, mating was broken by resuspension in 2 mL LB. Next, 100 µL and 20 µL of the bacterial suspension was plated on LB agar plates containing irgasan (25 µg/mL) and Gm (75 µg/mL), for the selection of merodiploids, and incubated overnight. Four colonies were chosen for each gene and streaked on LB plates and incubated for about 72 hours at room temperature, a reasonable amount of bacteria was then scraped and grown overnight at 37°C in LB plates with 20 % sucrose (Sigma Aldrich #S7903). To achieve the second crossover, counter selection on no-salt lysogeny broth (NSLB) agar containing 15 % sucrose was performed (Sigma Aldrich #S7903). For this, bacteria were picked, plated and grown overnight at 37°C. Finally, the loss of the plasmid was tested by streaking colonies on LB agar plates containing Gm (75 µg/mL)

and in parallel on LB agar plates without antibiotics. Single colonies were picked and streaked with the same tip on both plates, which were then incubated overnight at 37°C. The colonies that didn't grow on the Gm containing plate were chosen for its correspondent colonies on the LB plate to be scrapped and resuspended in 50 µL of purified water. The samples were then heated at 95°C for 5 minutes in a Thermomixer Comfort (Eppendorf) and centrifuged at 4500 rpm for 5 minutes, to be subsequently analyzed by PCR. The PCRs were executed according to the MangoMix protocol (described in tables 11 and 12). In-frame deletion mutants were confirmed by PCR using first a primer pair flanking the target gene (forward and reverse primers) and secondly a primer pair where one primer binds to the coding region of the target gene (forward and inside primers).

2.2.2. Growth curves

The increase in cell size and cell mass during the development of an organism is called growth. Each species has its own, unique, growth curve, although the same phases are reached, each species takes different times and reach higher or lower optical densities (ODs) to go through the same four phases of growth in a given medium, temperature and atmosphere - the lag phase, the exponential phase, the stationary phase and the death (which may also involve lysis) phase, as seen on the graphic representation on figure 6.

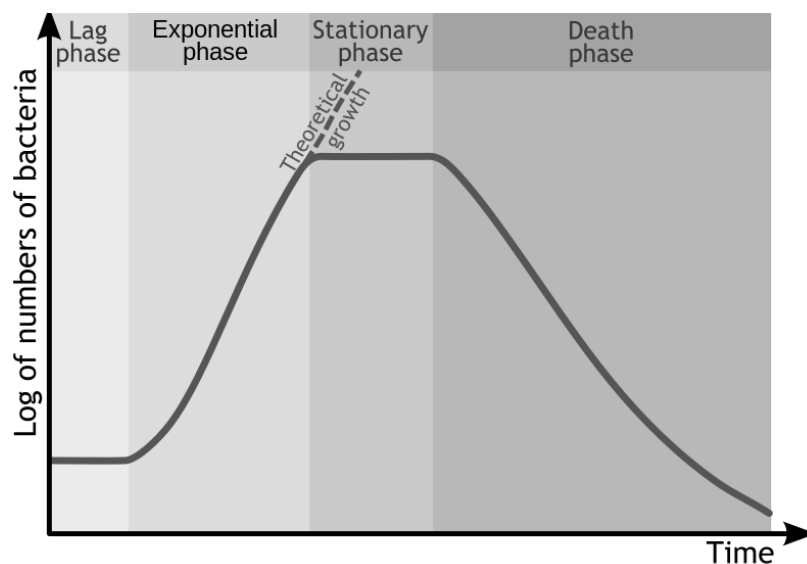


Figure 6 - Graphic representation of typical bacterial growth curve in culture medium.

Adapted from the illustration by Michal Komorniczak (26)

The organism requires certain basic conditions for energy generation and cellular biosynthesis, with its growth being affected by both physical and nutritional factors. The physical factors include the pH, temperature, osmotic pressure, availability of gases, among others, of the medium in which the organism is growing. The nutritional factors include the energy source and the source of carbon, nitrogen, sulphur, phosphorous, and other trace elements provided in the growth medium. In the assays performed the carbon source was changed according to the desired result, with experiments in which either glucose or sodium pyruvate were used as a carbon energy source, depending on the medium.

Bacteria are unicellular organisms. When the bacteria reach a certain defined size, they divide by binary fission, in which the one cell divides into two before continuing increasing in size. Such bacterium is then in a growing phase.

To study bacterial growth, bacteria of a species must be inoculated into sterile broth and incubated under optimal growth conditions. The bacteria start using the components of the media and will increase in size and cellular mass. The dynamics of the bacterial growth can be studied by plotting cell growth and division (for instance using the proxy measurement of absorbance/optical density) *versus* time. The spectrophotometer measures the optical density which is a measure of the amount of light absorbed by the bacterial suspension. The optical density is directly related to the size and number of microorganisms present and, as so, it is a convenient and rapid method to follow bacterial growth. The absorbance value increases as the amount of transmitted light through broth decreases due to increases in total cell mass. (27)

For the growth curves, 250 μ L of overnight culture were pipetted into a 14 mL round-bottom tube with 5 mL of LB medium. The diluted cultures were transferred into cuvettes, and optical density (OD) was measured using a photometer (BioPhotometer, Eppendorf) at a wavelength of 600 nm. Depending on the OD value obtained, calculations were performed to obtain a culture with a final OD value of 0.01. 1 mL of this culture was transferred into a well of a transparent 24-well-plate.

The growth was monitored over a 36 hour time period using the Tecan reader infinite 200[®] PRO (Tecan).

2.2.3. Determination of Minimal Inhibitory Concentrations (MIC Assay)

Minimum inhibitory concentrations (MICs) are defined as the lowest concentration of an antimicrobial that inhibits the visible growth of a microorganism after overnight incubation, they are considered the gold standard for determining the susceptibility of organisms to antimicrobials and are therefore frequently used in laboratories to confirm unusual resistance and to give a definitive answer when a borderline result is obtained by other methods of testing. (28)

To determine the MIC values of the generated mutants in comparison to the wildtype strain Pa ID40, microbroth dilution assays were performed using commercial kits as described next. This allows for the determination of the impact of the deleted genes on resistance to each antimicrobial tested and therefore predict the genes' involvement in the resistance mechanisms of Pa.

For this assay a plastic loop was used to scrape a small amount of bacterial culture from a LB agar culture plate incubated for about 12 h to 16 h at 37°C, which was then submerged in 1 mL NaCl 0.9 % in small cell culture tubes (5 mL round bottom tubes). Then each tube was vortexed, and the McFarland value was measured in the DensiCheck plus (BioMérieux) aiming for a McFarland of 0.5. The value was adjusted by adding NaCl 0.9 %, vortexing, measuring and repeating until the correct value was achieved. 62.5 µL of the adjusted McFarland bacterial suspension were then added to 50 mL Falcons filled with 15 mL of Mueller Hinton Buillon medium (MHB) and homogenized. Commercial plates by Thermofisher and Merlin were used. 50 µL of inoculated MHB were pipetted into each well of GN2F and EUX2NF MIC plates (Thermofisher) and 100 µL into each well of MICRONAUT-S β-Lactamases plates (Merlin). Each plate was sealed individually with the provided foil and then incubated for 18 h to 24 h at 37°C without shaking, the plates were incubated stacked but no more than 5 plates were ever stacked. After incubation OD at 600 nm was measured using the Tecan reader, if the OD value was inferior to 0.2 the bacteria were considered sensitive.

For the MIC measurement of fosfomicin an E-test was done. Using a plastic loop a small amount of bacterial culture was scraped from a LB agar culture plate, incubated for about 12 h to 16 h at 37°C. Physiological sodium chloride solution was then inoculated to a McFarland

standard of 0.5 with said loop. From this solution, bacteria were streaked over the entire agar surface with sterile cotton swabs onto Mueller-Hinton agar plates. One fosfomycin [0.064 - 1024 µg/mL] MIC test strip (Liofilchem) was then applied in the center of each plate. The plates were then incubated for 18 h to 24 h at 37°C. After this, the MIC value was read where the edge of the inhibition ellipse intersects the side of the strip.

2.2.4. Efflux activity assay

In order to eliminate antimicrobials, many MDR bacteria use a similar resistance mechanism, the overexpression of efflux-pumps. (29)

The goal of the efflux activity assay was to understand if the efflux pumps played a role in increasing the resistance of mutant strains compared to the wild-type strain. For this assay Hoechst 33342 was used. Hoechst 33342 is a dye that passes through the bacterial cell envelope and binds to double stranded DNA, resulting in the emission of blue fluorescence that is then measured. (30) It is also a substrate for a variety of efflux pumps also mediating resistance to antimicrobials, as well as a multitude of multidrug resistance transporters. (30–32)

To perform the efflux activity assay, subcultures of overnight cultures were grown for 2 to 3 hours in LB medium, they were then centrifuged at 4495 g for 5 minutes, and the pellet suspended in 3 mL PBS. The OD was then measured and adjusted to 0.3 with PBS. 180 µL of the adjusted OD culture suspension were then added into each well of a black 96-well plate with flat bottom in duplicates. Dulbecco's PBS duplicates were also made and used as blank. 20 µL of Hoechst 33342 from Thermo Fisher Scientific (100 µM) were added to each well immediately before placing the plate in the Tecan reader. For the fluorescence measurement the settings were the following: excitation light 355 nm; emission measurement 460 nm; flashes per well 7, measurements per well 3x3; interval of measurement 60 s; number of cycles 60.

2.2.5. Beta-lactamase activity

Beta-Lactamases are a large family of hydrolases capable of hydrolyzing β -lactams. β -lactam antibiotics (such as penicillins, cephalosporins and carbapenems) are highly susceptible to being hydrolyzed by enzymatic activity, deactivating their antibiotic potency. The beta-lactamase activity assay detects and quantifies the enzymatic activity of these hydrolases. The hydrolysis of a chromogenic cephalosporin, Nitrocefin, generates a coloured product (OD 490 nm) proportional to the amount of β -lactamase activity. One unit of β -lactamase is the amount of enzyme required to hydrolyze 1.0 μ mole of nitrocefin per minute at pH 7.0 at 25°C. Enzymatic activity as low as 0.06 mU can be detected by this assay. (33,34)

For the β -lactamase activity assay the β -Lactamase Colorimetric Assay Kit (BioVision) was used. The overall protocol of the kit was followed with minor alterations, as follows.

The bacterial strains were grown overnight, and the bacteria were subcultured with a 1:20 dilution in 20 mL LB for 3 hours. One sterile 1.5 mL Eppendorf per strain was pre-weighted. After the assay components were thawed at room temperature (assay buffer, hydrolysis buffer and nitrocefin), the bacteria were centrifuged at 4500 g for 5 minutes at room temperature. Then the supernatant was decanted, and the bacteria resuspended in the remaining liquid (100 μ L - 200 μ L) following with another centrifugation step for 10 minutes at 10000 g, the supernatant was then removed and discarded. The samples were then centrifuged again for 1 minute at 10000 g and the supernatant was, once again completely removed and discarded. The Eppendorf tubes were weighted with the pellet in order to calculate the weight of the same. The pellet was then resuspended in 20 μ L assay buffer per mg of pellet. The suspension was then sonicated with Sonorex Super RK 510 sonicator (Bandelin) on ice for a total time period of 5 minutes. The samples were then centrifuged at 16000 g for 20 minutes at 4°C.

The hydrolysed nitrocefin for the standard was prepared by mixing 28 μ L DMSO, 8 μ L hydrolysis buffer and 4 μ L nitrocefin, and incubated at 60°C for 10 minutes, then cooled to room temperature. The nitrocefin standard was prepared by pipetting 0, 2, 4, 6, 8 and 10 μ L of hydrolysed nitrocefin and adding assay buffer to 100 μ L total volume in a transparent flat 96-well plate in order to obtain a standard curve. The Reaction Mix was prepared by mixing 48 μ L of assay buffer with 2 μ L of nitrocefin per sample. The supernatant was diluted in assay

buffer, the dilution was 1:50 (1 μ L supernatant was added to 49 μ L assay buffer). Duplicates were used. 50 μ L of reaction mix were added per well and measured immediately at the Tecan reader, and the following settings were used: absorption at 490 nm, measured every minute for 1 hour, one measurement in the middle of the well. The beta-lactamase activity values were then calculated using the described procedure on the manufacturer's protocol. The 0 standard reading is subtracted from all readings, then the Nitrocefin Standard Curve is plotted, and two time points are chosen (T1 & T2) in the linear range to calculate the beta-lactamase activity for each sample. The Δ OD is calculated by Δ OD = A2 - A1, at a linear region of the curve. The Δ OD is then applied to the Nitrocefin Standard Curve to get B nmol ($Y = mX + B$) of hydrolyzed Nitrocefin generated by β L during the reaction time ($\Delta T = T2 - T1$).

$$\text{Sample } \beta\text{L Activity} = B/(\Delta T \times V) \times D = \text{nmol}/\text{min}/\text{mL} = \text{mU}/\text{mL}$$

Where: B is the amount of Nitrocefin from the Standard Curve (nmol)

ΔT is the reaction time (min.)

V is the sample volume added into the reaction well (mL)

D is the sample dilution factor

2.2.6. mRNA expression

To investigate whether the higher susceptibility to β -lactam antibiotics results from a reduced expression of the *ampC* gene, it is important to quantify the expression level of *ampC*.

Nuclease-free water (Invitrogen), LoBind Eppendorf tubes and RNase-free filtered pipette tips were used when handling RNA.

2.2.6.1. RNA isolation

For RNA isolation the ZymoBIOMICS RNA Miniprep Kit from ZYMO Research was used and its protocol was followed with some alterations. Unless otherwise stated centrifugations were done at 10000 g to 16000 g for 30 seconds.

The sample preparation part of the protocol started with the subculture of overnight cultures with 1:20 dilution (250 μ L in 5 mL LB) for 2 to 3 hours followed by a centrifugation step at 4495 g for 5 minutes. Then the pellet was resuspended in 500 μ L water and transferred

to an Eppendorf tube and then submitted to a centrifugation at 10000 g for 1 minute. The process was then repeated, finally the pellet was resuspended in 100 μ L water and then transferred to a ZR BashingBead Lysis Tube where 750 μ L of DNA/RNA Shield solution were added. The Eppendorf tubes were then shaken at maximum speed for 20 minutes. The samples were then centrifuged at 10000 g to 16000 g for 1 minute and the supernatant of each sample was transferred into two Eppendorf tubes with a volume of 200 μ L each.

The RNA purification part of the protocol follows, starting with the addition of 2-fold (400 μ L) RNA Lysis Buffer, followed by the addition of 1-fold (600 μ L) ethanol (95 % - 100 %) and mixing. Both tubes are then processed in one column by transferring 800 μ L into a Zymo-Spin IIICG Column in a Collection Tube, centrifuging at 10000 g to 16000 g for 30 seconds, discarding flow-through and repeating the process 3 times (until the total volume of each sample is processed in a column). Then 400 μ L of RNA Prep Buffer is added to the column which is centrifuged and the flow-through discarded. Next, 400 μ L of RNA Wash Buffer are added into the column, which is again centrifuged, the flow-through is now carefully transferred into a RNase-free tube. 88 μ L of water are then added to the column which is subsequently centrifuged. Next, 1 μ L of RNasin, 10 μ L of DNA Digestion Buffer and 1 μ L of DNase I are added to the sample and gently mixed. The samples are then incubated at 37°C for 20 minutes. After the incubation period, 200 μ L of RNA Lysis Buffer is added and mixed into the samples, followed by 300 μ L of ethanol, which suffers the same procedure. The whole mix is transferred to Zymo-Spin IIICG Column in a Collection Tube and centrifuged, and the flow-through is discarded. 400 μ L of RNA Prep Buffer are then added to the column which is centrifuged and the flow-through discarded. This process is repeated with 700 μ L of RNA Wash Buffer and then again with 400 μ L however this time the centrifugation step lasts 2 minutes and subsequently the column is carefully transferred into a RNase-free tube. Next, 50 μ L of water are directly added to the column which is then centrifuged. A Zymo-Spin™III-HRC Filter is prepared by adding 600 μ L of ZymoBIOMICS™HRC Prep Solution into it and centrifuging it at 8000 g for 3 minutes. This column is then transferred into a new, empty RNase-free tube. The eluted RNA (eluted previously with 50 μ L of water) is transferred into the previously prepared Zymo-Spin™III-HRC Filter in the RNase-free tube and centrifuged at exactly 16000 g for 3 minutes.

To verify sample quality, concentration was measured at a nanodrop when the protocol was finished, before storing RNA.

2.2.6.2. qPCR (quantitative Polymerase Chain Reaction)

Unlike a conventional PCR, qPCR amplifies nucleic acids but also quantifies them, in order to do this, a dye that intercalates with nucleic acids is used and its fluorescence is measured. (35) The fluorescence of the dye increases proportionally with the amount of PCR products. (35) The point of the qPCR is to determine the samples' quality, verifying there's no DNA in them, which would alter the expression results of the qRT-PCR assay.

For the qPCR, diluted digested RNA (1:10) was used and always kept on ice. The primers used were previously prepared for the research group for the Pa *gyrB* gene (table 8). The used mastermix was prepared using 5 μ L 2xSYBR-Green-RT-PCR-Mastermix (Qiagen, Hilden), 1 μ L forward primer, 1 μ L reverse primer, 2 μ L purified H₂O, which totals a volume of 9 μ L per reaction. A white 96-well qPCR plate is then filled with 9 μ L of mastermix per well, on ice, and 1 μ L of diluted RNA template is added according to scheme and mixed by pipetting. The plate is then closed with foil and the plate is shortly centrifuged (approximately at 200 g). The plate is then inserted in the Light Cycler 480 II (Roche) where quantitative absorbance is measured. The same program was used for the qPCR and for the qRT-PCR, as follows: reverse transcription at 50°C for 10 minutes, PCR initial activation step at 95°C for 5 minutes, and 40 cycles of denaturation at 95°C for 10 seconds followed by combined annealing/ extension at 60°C for 30 seconds.

2.2.6.3. qRT-PCR (Reverse transcriptase Real-time PCR)

The quantification of *ampC* expression was this assay's goal. For this, SYBR Green RT-PCR Kit (QIAGEN, no. 204154) was used according to manufacturer's instructions, using SYBR Green I as dye. This Kit includes a reverse transcriptase (RT-enzyme) that generates complementary DNA (cDNA) from the RNA template. The primers used were previously established by Klein *et al.* by generation of a standard curve by dilution of one sample and calculation of the efficiency of the PCR. (36) According to these results, the efficiency value of *gyrB* was 2.363 and of *ampC* was 2.480, and these were the efficiency values used.

For the qRT-PCR, diluted digested RNA (1:10) was used and always kept on ice. The primers used were previously prepared for the research group (table 8). The used mastermix was prepared using 5 μ L 2xSYBR-Green-RT-PCR-Mastermix (Qiagen, Hilden), 1 μ L forward primer, 1 μ L reverse primer, RT Mix Enzyme 0.1 μ L, 1.9 μ L purified H₂O, which totals a volume of 9 μ L per reaction. A white 96-well qPCR plate is then filled with 9 μ L of mastermix per well, on ice, and 1 μ L of diluted RNA template is added according to scheme and mixed by pipetting. The plate is then closed with foil and the plate is shortly centrifuged (approximately at 200 g). The plate is then inserted in the Light Cycler 480 II (Roche) where quantitative absorbance is measured. The same program was used for the qPCR and for the qRT-PCR, as follows: reverse transcription at 50°C for 10 minutes, PCR initial activation step at 95°C for 5 minutes, and 40 cycles of denaturation at 95°C for 10 seconds followed by combined annealing/ extension at 60°C for 30 seconds.

To analyze RNA expression, the quantification of RNA is needed, and it is obtained through calculations, using the Pfaffl mathematical model, a method which uses gene's efficiency and is normalized to the reference housekeeping *gyrB* gene. (37) This method provides relative quantification of the transcript of the target gene in comparison to the housekeeping reference gene. Housekeeping genes are typically expressed at a relatively constant rate and mainly encode for proteins important for the preservation of basic cell functions, hence are often used to normalize mRNA levels. (38) For this method it's also necessary to obtain the crossing points (CP) measured during the PCR. The CP is the cycle number where the fluorescence measured it's at its highest rising rate crossing the threshold line, which is determined by the LightCycler® 480 Software. (39)

2.2.7. Serum killing

An important first line host defense against invading bacteria specifically in bloodstream infection is the serum complement system. (40,41) The goal of this assay was to measure the impact of the genes on resistance against the complement system components. The cell viability is measured in this assay instead of cell density, which is measured in other assays such as in growth curves.

To perform the serum killing assay subcultures of overnight cultures were grown for 2 to 3 hours in LB medium. The subcultured bacteria were then centrifuged for 5 minutes at 4500 g and the pelleted bacteria resuspended in 1 mL PBS. For measuring the OD, at 600 nm, 100 μ L of each bacterial culture were added in a cuvette with 900 μ L PBS, and a PBS filled cuvette was used for blanking. With the OD values the bacterial concentration can be calculated. Since an OD at 600 nm of 1 equals 10^9 bacteria per mL, this means: $OD \times \text{dilution factor} (10) \times 10^9 = \text{Bacteria/mL}$. This information is necessary to calculate the volume of human serum necessary for the assays, as well as the volume of bacterial solution needed.

The BacTiter-Glo™ Reagent used in this assay was always made freshly before each assay following manufacturer instructions (BacTiter-Glo™ Microbial Cell Viability Assay, Promega).

Two different sets of serum were prepared: normal human serum (NHS) and inactivated human serum (HIS), these two serums were then used in different concentrations. The normal human serum (NHS) is from healthy donors (Transfusion medicine, University hospital Tübingen) and was stored in aliquots at -80°C . The NHS was simply thawed quickly in a 37°C water bath and kept on ice. The HIS was heat inactivated in a water bath at 56°C for 30 minutes after thawed and then kept on ice.

A stock solution containing the final bacterial amount of 5×10^6 bacteria per well was prepared for each strain. 50 μ L of bacterial suspension were pipetted into each well of V-bottom 96-well plates according to the experiment layout.

Luminescence (cell viability) was measured at different time points in order to get a better understanding of the impact of the genes on the resistance of the bacteria to the human serum.

At the starting point no human serum is added, 50 μ L of PBS is added to each well and the shaking time is reduced to 5 minutes, otherwise standard protocol applies. The standard protocol for all other time points is then as follows. The measurement, after 1 hour, 2 hours or 4 hours, in normal human serum (NHS) or heat inactivated serum (HIS) is done by pipetting for each strain 50 μ L aliquots ($10^8/\text{mL}$) in three wells (triplicates), of a 96-well plate, the appropriate volume of HIS or NHS. PBS to a final volume of 100 μ L is then added and the mix is resuspended. Each plate is incubated at 37°C for the determined incubation period. After incubation, the plates are centrifuged for 5 minutes at 3500 g, the supernatant is poured off and 100 μ L of PBS is added to each well.

50 μL of this bacteria/serum mix from each well is then transferred to a white 96-well plate and 50 μL of BacTiter-Glo™ Reagent is added in each well. The plates are then shaken for 10 minutes and then the luminescence signal is read using the Tecan reader.

The BacTiter-Glo™ Assay System utilizes a proprietary luciferase to enable extraction of ATP from bacterial cells and allows for a uniform “glow-type” luminescent signal. The luminescent signal read is proportional to the quantity of ATP present, and the ATP is directly proportional to the number of cells alive in the media.

3. Results and Discussion

Pa uses the peptidoglycan recycling pathway in order to recycle cell-wall components, a process essential for resource conservation for the extensive cell-wall remodeling that *Pa* endures. (13) The genes *amgK*, *anmK*, *mupP* and *murU*, were shown to be involved in this pathway. (18) According to a previous study it was hypothesized that these genes contribute to beta-lactam resistance. (10) For two further genes namely, *bepA* and *ycgE2* it was hypothesized that these also contribute to beta-lactam resistance. While *BepA* is a periplasmic Zinc-metalloproteinase that is involved in the maintenance of outer membrane integrity (42), *YcgE2* is a helix-turn-helix-type transcriptional repressor (GenBank: VVH84782.1).

By generating deletion mutants as described in “2.2.1 Generation of deletion mutants”, validation of *amgK*, *anmK*, *mupP*, *murU*, *bepA* and *ycgE2* involvement in beta-lactam resistance was the goal.

3.1. Generation of deletion mutants

The genes *bepA*, *murU*, *mupP* and *ycgE2* were identified in the TraDIS screen described in Sonnabend *et al.* (10). To validate the identification of these genes by the TraDIS analysis and investigate whether these genes are relevant to *Pa* antibiotic resistance it is necessary to begin by generating *Pa* ID40 Δ *bepA*, Δ *murU*, Δ *mupP* and Δ *ycgE2* deletion mutants.

To generate the desired deletion mutants Gibson Assembly (described in extensive detail in the Methods section) was used in order to obtain plasmids that would target the chosen genes. Gibson Assembly allows for successful assembly of multiple DNA fragments, regardless of fragment length or end compatibility, efficiently joining multiple overlapping DNA fragments in a single-tube isothermal reaction. The Gibson Assembly Master Mix includes three different enzymatic activities that can occur in a single buffer: The exonuclease creates single-stranded 3' overhangs that facilitate the annealing of fragments that share complementarity at one end (overlap region); the proprietary DNA polymerase fills in gaps

within each annealed fragment; and the DNA ligase seals nicks in the assembled DNA. The end result is a double-stranded fully sealed DNA molecule that can serve as template for PCR and direct transformation. (Fig. 7) The method has been successfully used to assemble from small oligonucleotides, larger DNA fragments with varied overlap lengths (15–80 bp,) to fragments hundreds of kilobases long. (23,43)

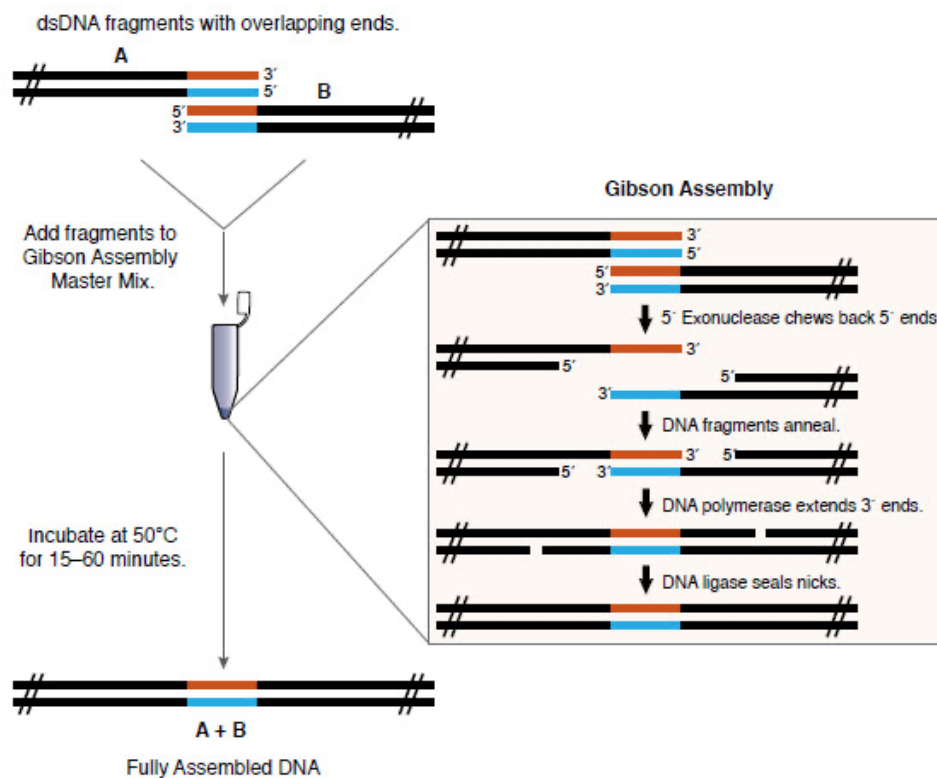


Figure 7 - Overview of the Gibson Assembly Cloning Method.

Method of cloning two or more fragments in which user-defined overlapping ends are merged into the fragments allowing for seamless incorporation of adjacent fragments. (23) At a temperature of 50°C, a 5'-exonuclease acts in order to remove the 5'-ends of each strand of the double-stranded DNAs (dsDNA), A and B, allowing the overlap and consequent annealing of the 3'-ends. The extension of the 3'-end regions by a DNA polymerase and sealing of the nicks by a DNA ligase, lead to the origin of the fully assembled DNA. Image from BioLabs' Gibson Assembly® Cloning Kit Manual. (44)

Another very important step of the generation of deletion mutants is the conjugation, during which the genetic material is transferred from the donor bacterium to the recipient bacterium once in direct contact. The genetic material transferred is commonly a plasmid and it can confer novel genes to the recipient bacteria which may result in changes of phenotype,

such as expression of antibiotic resistance. DNA regions of hundreds to thousands of kilobases can be transferred. It's also worth mentioning that conjugation is thought to have the broadest host range for DNA transfer among the methods of genetic exchange in bacteria. (24,25) In this thesis the desired DNA sequence is firstly achieved in *E. coli* SM10 λ pir and is then transferred into Pa ID40 using conjugation.

Finally, in order to confirm the deletion mutants, the method depicted in Fig. 8 was used. Two PCRs were performed independently. In the first reaction, the primers bind to the flanking regions of the gene (denominated in this thesis as forward and reverse primers), and in the second, one primer binds to the flanking region while the other binds to the coding region (denominated in this thesis as forward and inside primers). In the first PCR a smaller product should be obtained for isolates with the gene deletion than those who maintained the wildtype. In the second PCR, no product should be observed for the isolates who present the deletion.

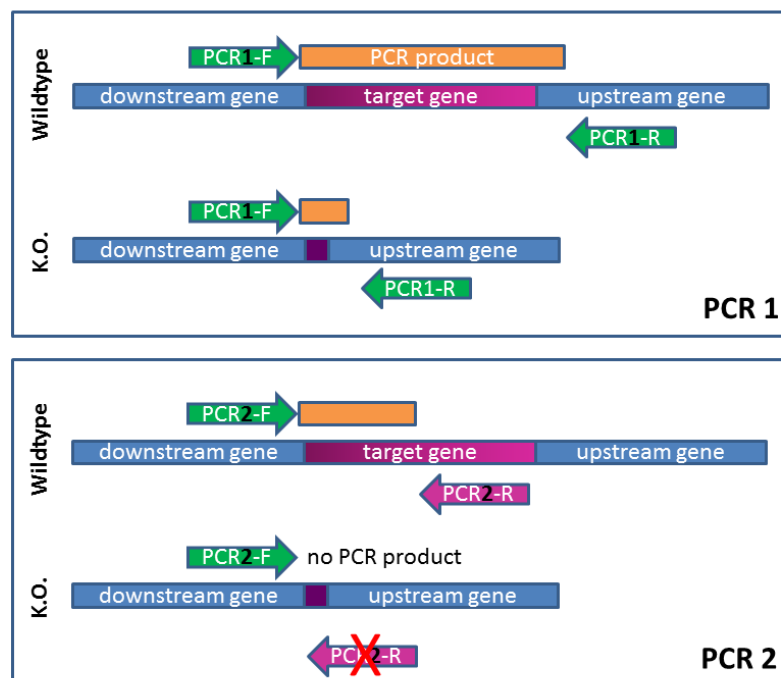


Figure 8 - Identification of deletion mutants by PCR.

Discernment of deletion mutants was accomplished by the application of two PCRs. PCR1: The primers bind in the flanking region of the gene. This should result in a smaller PCR product for the colonies where the gene deletion occurred than in those that reverted to the wildtype. PCR2: One primer binds to the flanking region of the gene and the other primer binds directly to the coding region. Only in isolates that reverted to the wildtype will there be a DNA product amplified. A mutant was confirmed only if both PCRs demonstrated the appropriate results. Primers that bind to the flanking region of the gene (green) or directly to the coding region (purple) are represented by arrows. PCR: Polymerase Chain Reaction; F: Forward; R: Reverse; K.O.: knockout/ deletion mutant. Image from Bohn *et al.* Unpublished.

The expected sizes for the PCR products are listed in table 13. The agarose gels with the results of each PCR are presented in figures 9 and 10.

Table 13 - Calculated size of PCR products, in base pairs (bp), according to the primers used in the PCR.

Gene	Primers used	Size of WT product (bp)	Size of mutant product (bp)
<i>murU</i>	994/995	821	445
	994/996	335	–
<i>mupP</i>	1001/1002	1041	352
	1001/1003	391	–
<i>bepA</i>	1015/1016	1606	352
	1015/1017	352	–
<i>ycgE2</i>	1022/1023	676	379
	1022/1024	284	–

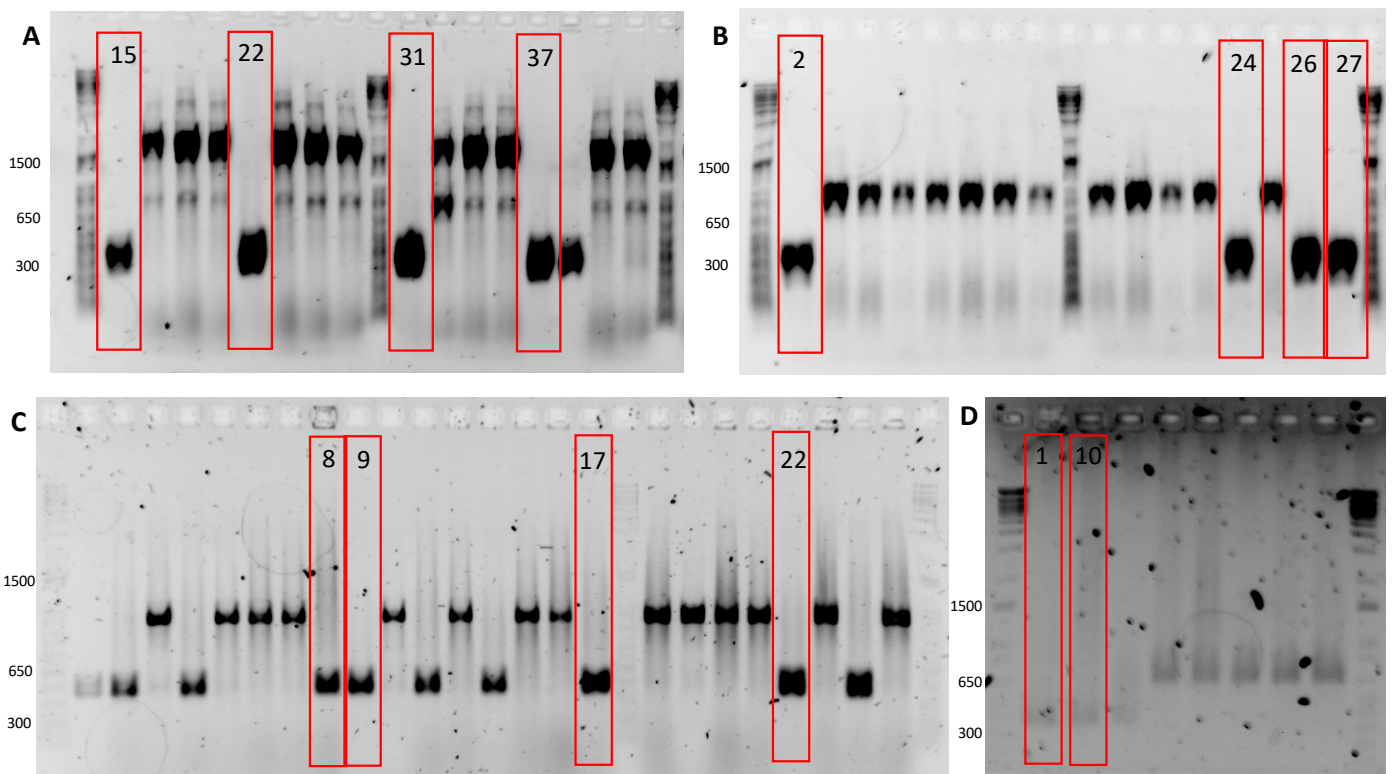


Figure 9 - Agarose gel 1 % electrophoresis of the colony-PCR products.

PCR was performed using the forward and reverse primers of each gene selected for deletion (*bepA*; *mupP*; *murU*; *ycgE2*). In (A), (B), (C) and (D) clones of *bepA*, *mupP*, *murU* and *ycgE2* mutants were loaded and run in an agarose gel. The first well of each gel corresponds to the Gene Ruler 1 kb Plus DNA ladder (100 – 15.000 bp). In the red rectangles, the positive putative mutants chosen to move forward are identified. The number in each rectangle represents the ID of the clone chosen. On the left of each gel the numbers are in base pairs.

Figure 9 shows the results from the first polymerase chain reaction, where the forward and reverse primers were used. From this reaction, a smaller product should be obtained for isolates with the gene deletion than those who maintained the wildtype, the specific sizes are identified in table 13. Thus, for the isolates without the deletion of the *murU*, *mupP*, *bepA* and *ycgE2* genes, a product size of 821 bp, 1041 bp, 1606 bp and 676 bp, respectively, is to be expected. On the other hand, isolates that present the corresponding deletion, should present smaller products: 445 bp for *murU* deletion; 352 bp for *mupP* deletion; 352 bp for *bepA* deletion; and 379 bp for *ycgE2* deletion. Knowing this, and comparing to the results obtained in figure 9, we can see that the chosen clones, for each gene, present the expected band size. Indeed, for *bepA* deletion (figure 9 (A)), in the chosen clones 15, 22, 31, and 37, we see a band a little above the 300 bp. In the *mupP* putative mutants (figure 9 (B)), in the chosen clones 2, 24, 26, 27, we observe once more, a band a little above 300 bp. For the *murU* putative mutants, clones 8, 9, 17, 22 (figure 9 (C)) were chosen as they presented a band slightly under 500 bp. And lastly, for the *ycgE2* putative mutants, clones 1 and 10 (figure 9 (D)) were chosen, where a band size of around 400 bp is seen.

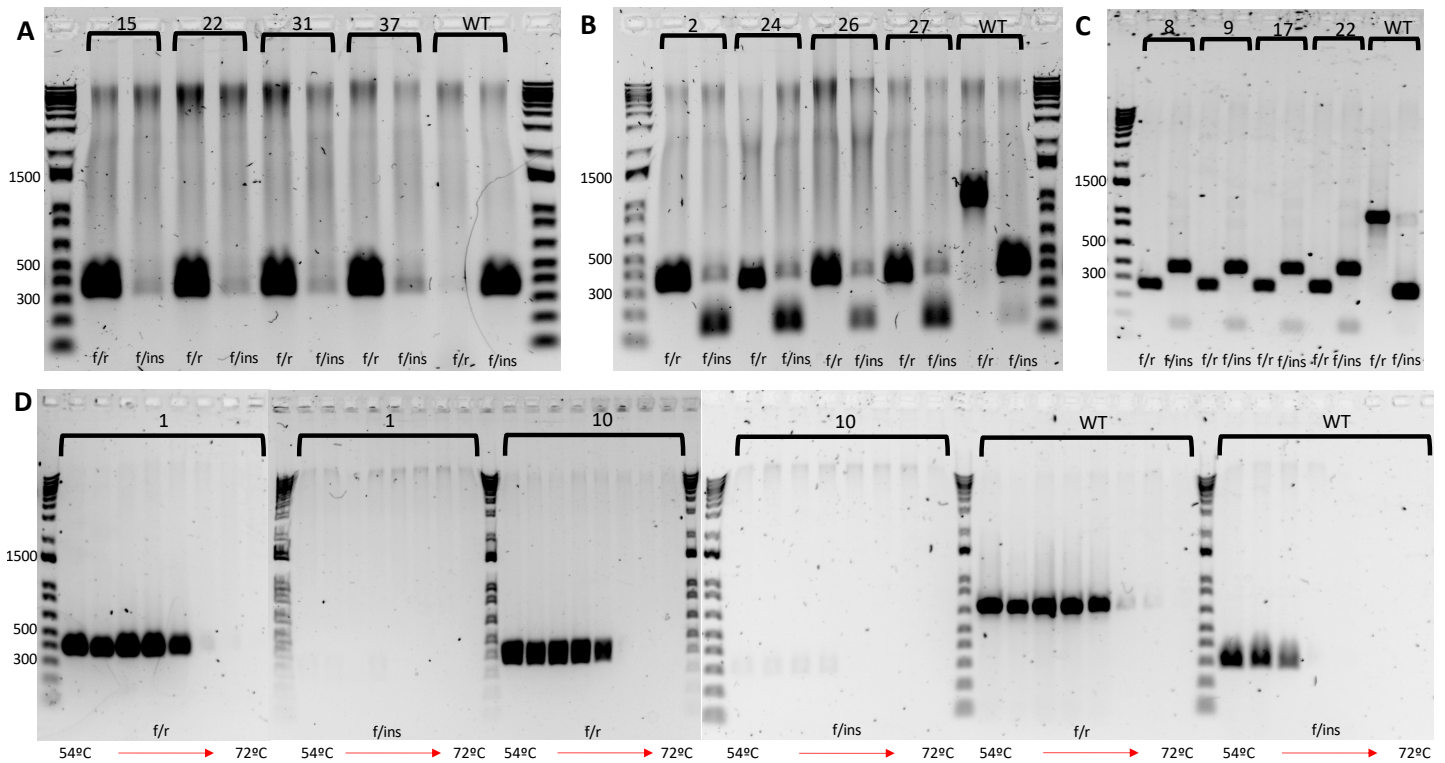


Figure 10 - Agarose gel 1 % electrophoresis of the colony-PCR products of the clones selected previously (Fig. 9).

PCR was performed using two different sets of primers: forward/reverse and forward/inside primers, of each gene selected for deletion (*bepA*; *mupP*; *murU*; *ycgE2*). In (A), (B), (C) and (D) clones of *bepA*, *mupP*, *murU* and *ycgE2* mutants were loaded and run in an agarose gel. The first well of each gel corresponds to the Gene Ruler 1 kb Plus DNA ladder (100 – 15.000 bp). For each clone, identified by the corresponding number, the results of the use of the forward/reverse primers are on the left. On the right, the results of the use of the forward/inside primers are presented. In (D) a PCR temperature gradient from left to right from 54°C to 72°C was applied. On the left of each gel the numbers are in base pairs.

With the putative deletion mutants selected, the second colony-PCR was performed (Figure 10) using the flanking primer and the primer inside the coding region. Here, the absence of a band in each mutant is to be expected, confirming that way the deletion of the gene of interest. In Figure 10 (A), for the *bepA* gene deletion, we can distinguish in the wells corresponding to the product resulting from the amplification with the forward and inside set of primers, the presence of a faint band. These faint bands are most likely nonspecific bands or primer-dimers. The same is seen for the clones in which *mupP* was deleted (Figure 10 (B)). Thus, in order to establish if the faint bands correspond to a portion of the gene of interest or are merely an artifact, a PCR with a temperature gradient (54°C - 72°C) was performed (results not shown). Here, a fading out of the bands in the mutant strains could be distinguished,

when compared to the WT, which indicated that the faint bands observed in Figure 10 (F/Ins wells) are indeed an artifact, possibly resulting from non-specific binding. Experimentation with annealing temperature or time could possibly solve this issue. In the same way, similar results for clones of the *ycgE2* mutant can be noted, where a fading out of the band is perceived (Figure 10 (D)). Finally, for the *murU* deletion clones (Figure 10 (C)), the presence of bands is also clear. However, since these bands are much stronger and well defined they were sent for sequencing which showed these bands represent a part of the gene PROKKA_01040 *puuA*. Thus, the presence of these bands are, once more, artifacts.

Overall, these results indicate a successful deletion of the *bepA*, *mupP*, *murU* and *ycgE2* genes.

Pa ID40 Δ *bepA*, Δ *murU*, Δ *mupP* and Δ *ycgE2* deletion mutants were successfully generated and used for further research.

3.2. Growth curves

3.2.1. Growth curves in LB medium

The first step to characterize the deletion mutants was to investigate whether deletion of the studied genes affects growth.

In order to explore the effects of the mutations on Pa ID40 in LB medium, growth curves were performed over a period of 36 hours. Differences in these curves can indicate deficiencies in different levels of the metabolism, as well as other disadvantages the lack of these genes may cause in fitness, such as implications in regulatory networks. Hence, the growth curves are the first step into the characterization of these genomic mutations in Pa.

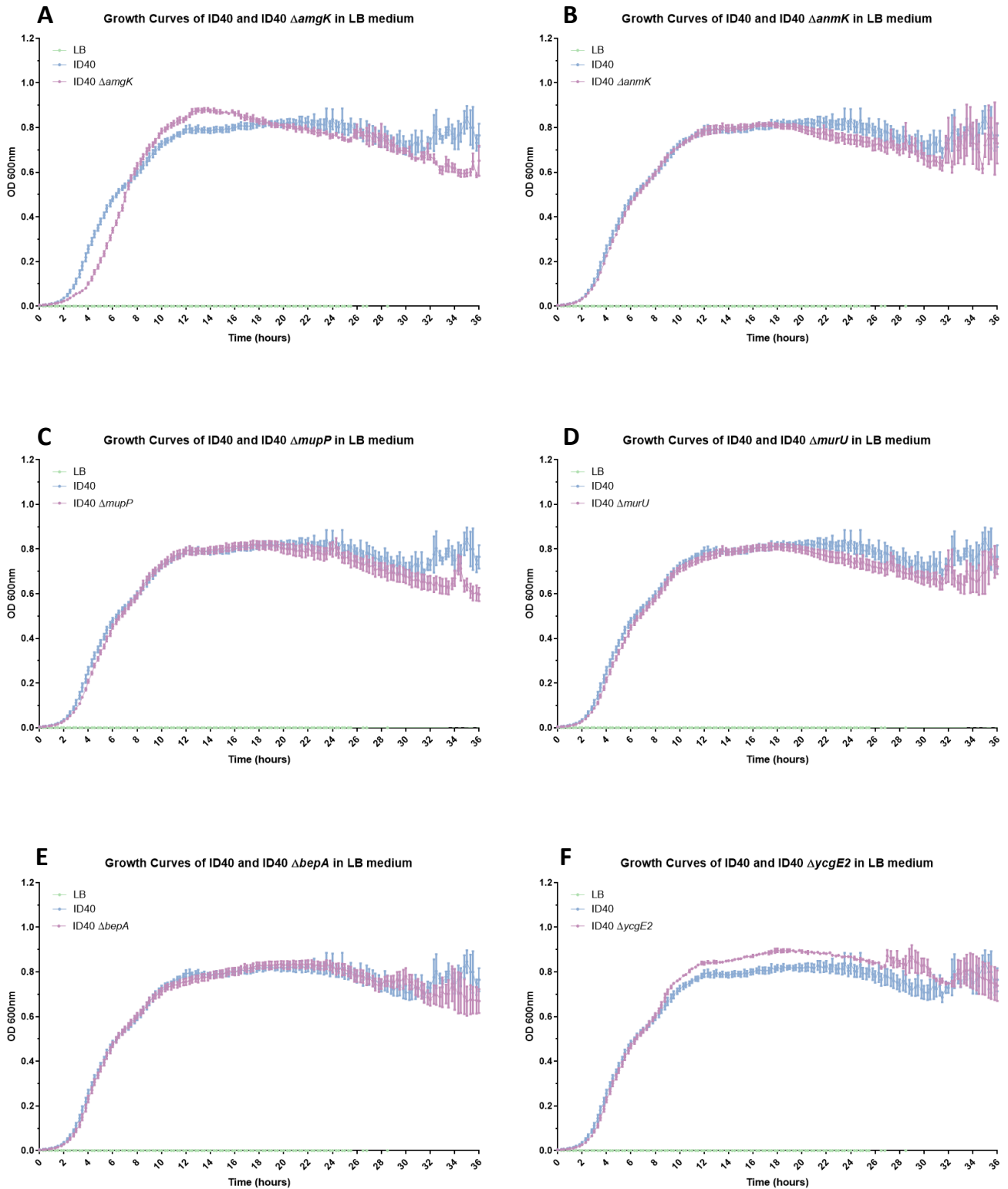


Figure 11 - Growth curves of *P. aeruginosa* ID40 strain and mutants ($\Delta amgK$, $\Delta anmK$, $\Delta mupP$, $\Delta murU$, $\Delta bepA$, $\Delta ycgE2$) in LB medium.

Bacteria were grown at 37°C for a period of 36 hours, and the OD was measured at 600 nm. The temporal course of the growth of the ID40 strain (blue) and of the mutants (light mauve) $\Delta amgK$, $\Delta anmK$, $\Delta mupP$, $\Delta murU$, $\Delta bepA$ and $\Delta ycgE2$ are depicted. LB medium was used as negative control (green).

In this set of experiments, no relevant difference is observed between the mutants' and WT's growth curves in a period of 36 hours.

Pa ID40 lag phase lasts for about 1 hour (Figure 11 (A-F)), this is the initial period of life when the bacteria are still adapting to the new environment, and are therefore not able to divide. Then, the bacteria enter the exponential phase, also known as log phase, which lasts approximately 11 hours reaching an OD of around 0.8 (Figure 11 (A-F)). This phase is characterized by cell division and cells are now rapidly multiplying. The stationary phase is then reached at around 12 hours, lasting for roughly 12 hours (until 24 hours) keeping the same general OD of about 0.8 (Figure 11 (A-F)). At this phase, some cells are still dividing while others begin to die at a rate that leads to the size of the population to remain constant. Finally, the bacteria enter the death phase at around 30 hours, the minimum OD that was read before the error became too big was of about 0.7 (Figure 11 (A-F)). When cellular waste builds up and the media is depleted of its nutrients the death phase occurs, while there still may be a few bacteria dividing, this phase is characterized by a net loss of viable cells. To note that, during this phase, the measuring error becomes very large due to the big amount of lysed bacteria in the media that interfere with the reading of the accurate optical density.

The same general behaviour as described for Pa ID40 (WT) was observed in all graphs for all mutants (Figure 11 (A-F)), except in the *amgK* mutant graph (Figure 11 (A)) where the mutant strain seems to take longer to reach stationary phase but reaches it with a slighter higher OD than the WT strain, maintaining this superiority for only about 10 hours. It is unclear at this point what causes this behaviour change. The *ycgE2* mutant (Figure 11 (F)) presents a similar and non-remarkable behaviour to the WT strain but, once it reaches the stationary phase, it maintains the OD slightly higher than that of the WT until death phase.

No other significant differences are observed between the other mutants and the WT. A possible explanation for this behavior is that the stress that the gene deletions puts on the cells is not big enough to affect them in the absence of other stress factors such as nutritional deficiencies or the presence of inhibitors or antimicrobial drugs. Knowing that these genes are thought to affect the recycling pathway these results are expected, seeing that the *de-novo* biosynthesis pathway is still available for the production of the building blocks essential to bacterial growth. Thus, the mutations in *amgK*, *anmK*, *mupP*, *murU*, *bepA* and *ycgE2* make

very little difference in the growth process, reflected by the lack of discrepancies between the presented growth curves.

Additionally, these results are similar to the ones obtained by Borisova *et al.* in 2014, where no difference was found between the wild-types used (PAO1 and PA14) and the *amgK*, *murU* and *anmK* deletion mutants, in the same media. (15) This reiterates the already expected results. Furthermore, a study by Park and Uehara *et al.* in 2008 in *E. coli* noted that since PG is not a substantial source of nutrients, recycling only provides the needed building blocks to continue the normal cell cycle when an abrupt reduction of carbon in the media occurs. (44) With these results in mind, the same procedure was followed in carbon restricting conditions and growth curves were acquired using the M9 minimal medium.

3.2.2. Growth curves in M9 minimal medium

To achieve the bypass of the *de-novo* biosynthesis and force the PG recycling pathway bacteria were grown in M9 minimal medium, where sodium pyruvate is used as a carbon source instead of the glucose present in LB media. The absence of glucose in the media leads to the unavailability of fructose-6-P forcing the recycling pathway. Growth curves in this condition were acquired (Figure 12 (A-F)) and the results analyzed.

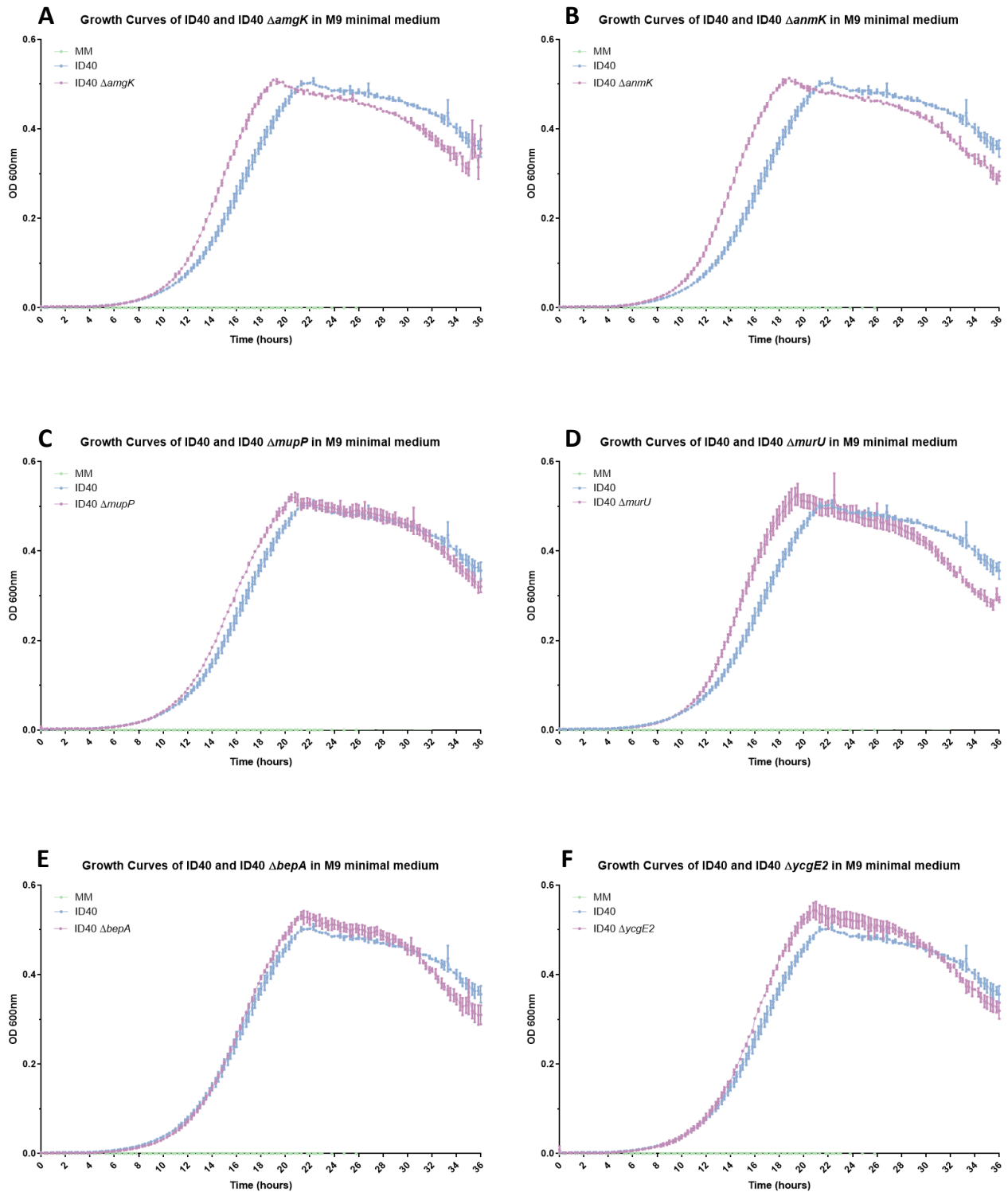


Figure 12 - Growth curves of *P. aeruginosa* ID40 strain and mutants ($\Delta amgK$, $\Delta anmK$, $\Delta mupP$, $\Delta murU$, $\Delta bepA$, $\Delta ycgE2$) in M9 minimal medium.

Bacteria were grown at 37°C for a period of 36 hours, and the OD was measured at 600 nm. The temporal course of the growth of the ID40 strain (light blue) and of the mutants (light mauve) $\Delta amgK$, $\Delta anmK$, $\Delta mupP$, $\Delta murU$, $\Delta bepA$ and $\Delta ycgE2$ are depicted. M9 minimal medium was used as negative control (green).

When the *de-novo* biosynthesis is blocked, and the recycling pathway is forced, all the growth curves showed a change from the growth curves in LB medium. In this set of curves, it's possible to observe differences between the WT and any mutant, although some are very insignificant while others are more noteworthy.

The *amgK*, *anmK*, and *murU* mutant growth curves exhibit the biggest difference from the WT growth curve, with a similar behavior between themselves, exiting the lag phase at around 5 hours and entering the stationary phase at around 19 hours, approximately 2 hours sooner than the WT (at about 21 hours), presenting a lower OD in the stationary phase that continues to diminish.

The *mupP* mutant strain's GC shows an analogous behaviour to the *amgK*, *anmK* and *murU* strains' GCs, however with a much smaller divergency to the WT's Gc in all growth phases, even having the same stationary phase OD as the WT.

Finally, *bepA* and *ycgE2* both show the same behaviour, with their growth curve phases coinciding with the WT's. In the *bepA* mutant growth curve the ODs appear to be similar to the WT's.

In most mutants the data (Figure 12 (A-D and F)) reflected a faster entrance into the stationary phase, which reflects a shorter exponential phase. This could be due to the mutants' lack of capacity to use the recycling pathway and therefore inability to conserve resources that leads to a quicker depletion of resources in the media and therefore early entry into death phase, when compared to the WT.

The final OD of all the mutant strains is always lower than the OD of the WT strain. A possible explanation for this phenomenon is that the mutants have a disadvantage in a nutrient depleted media. It is expected that the depletion of the media creates this disadvantage since they are not able to use the PG recycling due to the involvement of the deleted genes in the recycling pathway and there are no nutrients available for the *de-novo* biosynthesis.

The *mupP* mutant, which is expected to have an important role in the recycling pathway and in antimicrobial resistance according to Fumeaux *et al.* 2017 (19), didn't show a significant difference in these growth curves. This could mean either MupP has a homologue that can play its role with minimum disruption of the cell cycle, or that we have failed to fully activate

the PG recycling pathway and gluconeogenesis was activated to override the lack of fructose-6-phosphate, transforming the pyruvate into it, favoring the use of the *de-novo* pathway. To note that it's been described that no homologous exist of AmgK and MurU in Enterobacteria, even though they have been found in Proteobacteria, but no mention of MupP was found. (13)

3.3. Determination of Minimal Inhibitory Concentrations

To investigate the influence of the deleted genes in antimicrobial resistance, particularly in beta-lactam resistance, minimal inhibitory concentrations to a variety of antimicrobial drugs were assessed.

Antibiotics act on different points of the cell cycle, such as in protein synthesis and activity as well as cell-wall biogenesis and recycling. (13) Since the cell wall is exclusive to bacteria, it's extremely important to investigate how antibiotics act on its different components and their synthesis. Cell wall synthesis and recycling are the target for several commonly used antibiotics like beta-lactams, fosfomycin and glycopeptides. Hence, the components of the cell wall recycling play an essential role in resistance increase to these antibiotics. When evaluating the MICs of the different mutants this was taken into consideration and therefore, the observation of these, is expected to correspond to a difference in the roles of each gene on the cell wall recycling pathway and thus, as previously cited, in resistance. Importantly, some cell wall recycling components additionally participate in development of cross-resistance to other classes of antibiotics like fluoroquinolones, aminoglycosides and macrolides. (13)

Table 14 - Susceptibility of ID40 WT and deletion mutants against a variety of β -lactam, polypeptide and phosphonic antibiotics.

This table shows the MICs in $\mu\text{g}/\text{mL}$. The different shades of green represent the folds of resistance decreased in comparison to the WT (ID40). (1-fold for the lightest green, 3-fold for the most intense green). n.a: not available.

Antibiotic \ Strain	Strain						
	ID40	$\Delta anmK$	$\Delta amgK$	$\Delta mupP$	$\Delta murU$	$\Delta bepA$	$\Delta ycgE2$
Aztreonam	32	16	8	16	16	16	16
Cefepime	32	16	16	16	16	16	32
Ceftazidime	64	32	16	32	32	32	64
Doripenem	8	2	2	4	2	2	4
Imipenem	64	16	16	32	16	16	64
Meropenem	8	4	4	4	4	2	8
Piperacillin	128	128	64	128	128	128	128
Piperacillin/ tazobactam constant 4	128	128	32	128	n.a.	64	128
Polymyxin B	4	4	1	2	2	1	4
Fosfomycin	96	64	48	64	64	64	64

The *anmK* mutant presented resistance reduction to most of the antibiotics presented on table 14, including beta-lactams and phosphonic antibiotics, when compared to the WT strain, the exception being ureidopenicillins and polypeptide antibiotics, where no resistance reduction was observed. More precisely, this mutant demonstrated a decrease in resistance of 1-fold to aztreonam, cefepime, ceftazidime, meropenem and fosfomycin; 2-folds to doripenem and 3-folds to imipenem.

The *amgK* mutant exhibited the most decrease in resistance of all mutants, showing a reduction in resistance to all antibiotics, including ureidopenicillin and polypeptide antibiotics. Varying between a 3-fold reduction for imipenem, 2-fold for aztreonam, ceftazidime, doripenem, piperacillin with tazobactam, polymyxin B and fosfomycin, and 1-fold for cefepime, meropenem and piperacillin, when compared to the WT (table 14). These results may suggest a higher importance of this gene in the recycling pathway, pointing perhaps to a bigger impact on this pathway when compared to the other genes' proteins since

its resistance to all antibiotics presented is affected. More, this may also indicate that *amgK* is heavily involved in PG recycling, in cell wall stress, or most likely in both.

The *mupP* and *murU* mutants showed similar results, with a decline in resistance of 1-fold for aztreonam, cefepime, ceftazidime, meropenem, polymyxin B and fosfomycin, and slightly different results for imipenem, where *mupP* presents a 2-fold and *murU* presents a 3-fold decrease; and for doripenem where *mupP* presents a 1-fold reduction and *murU* shows a 2-fold reduction. This could mean the *murU* mutant strain is less resistant to carbapenems in general.

The *bepA* mutant shows a similar resistance decrease to the *murU* mutant except for meropenem (2-fold resistance reduction), piperacillin with tazobactam (1-fold resistance reduction), and polymyxin B (2-fold resistance reduction).

The *ycgE2* mutant showed almost no decreased resistance when compared to both the wild-type and the other mutants. Indeed, it only showed a decline in resistance of 1-fold to aztreonam, doripenem and fosfomycin. From these results alone one would conclude the *ycgE2* gene is most likely of insignificant importance in the resistance mechanisms of Pa.

There seems to be a pattern for resistance reduction in relation to the antibiotic, for instance, aztreonam and cefepime exhibit a 1-fold resistance reduction for almost all mutants, and piperacillin no reduction at all for nearly all mutants. Imipenem showed a big decrease in resistance across all mutants. This particularly big decrease of resistance in the presence of imipenem is interesting because imipenem is a beta-lactamase inducer and in its presence *ampC* expression is normally highly activated. (19,45)

As for the fosfomycin finding, it is in accordance with the literature, where it's well described how fosfomycin interacts with the recycling pathway, and how strains with the deletion of the recycling genes *mupP*, *murU*, *amgK* or *anmK* are hypersensitive to the antibiotic, showing a reduced MIC of at least 1-fold. (6,15,19)

Finally, for polymyxin B, since its mechanism of action consists of binding to LPS on the outer membrane thus increasing cell membrane permeability, resistance occurs when binding to LPS is hindered, by for instance target modification. (5) Susceptibility can be increased when the cell membrane is debilitated facilitating the increase of membrane permeability. For $\Delta amgK$ and $\Delta bepA$ a 2-fold decrease of MIC was observed for polymyxin B, possibly indicating these genes may be relevant in keeping membrane integrity. This is particularly

relevant for *bepA* since BepA has been described as having extensive roles in outer membrane maintenance. (42,46) BepA promotes proper OM assembly, degrades misassembled LptD (beta-barrel protein component of the lipopolysaccharide translocation channel), promotes LptD's maturation, amongst other functions which contribute to the maintenance of OM structural integrity. (42)

These findings are in accordance with the one's from Sonnabend *et al.* who also reported a decrease in antibiotic resistance for Pa ID40 Δ *amgK*. Moreover, the work of Sonnabend *et al.* suggested that the genes *amgK*, *anmK*, *mupP*, *murU*, *bepA* and *ycgE2* might contribute to meropenem and cefepime resistance in this same strain (Pa ID40). (10) This could be confirmed for all genes with the exception of *ycgE2*. In addition, all genes contribute more or less to beta-lactam resistance but to different antibiotics.

In normal conditions, UDP-MurNAc-pentapeptides binds to AmpR, repressing it. Once AmpR is repressed, it represses the *ampC* gene, leading to a decreased expression. In the presence of beta-lactams, 1,6-anhydro MurNAc peptides accumulate due to the inhibition of PG cross-linking by the PBPs, which cause the formation of uncross-linked glycans that are degraded by LTs into turnover products. The accumulation of 1,6-anhydro MurNAc peptides compete with the UDP-MurNAc-pentapeptides in the cytoplasm for binding to AmpR. Once 1,6-anhydro MurNAc peptides binds to AmpR it derepresses it, leading to an increase of *ampC* expression. (10,19)

It is hypothesized by Fumeaux *et al.*, that when the recycling pathway is disabled, due to the deletion of either *anmK*, *amgK*, *mupP* or *murU*, there's less amount of UDP-MurNAc-pentapeptides available to bind to AmpR. (19) One could think the PG *de-novo* biosynthesis pathway could compensate for the loss of UDP-MurNAc, derived from discontinue of the recycling pathway due to the mutations, by upregulating. However, according to Borisova *et al.* 2017, the PG *de-novo* biosynthesis pathway cannot compensate for this loss. (18) This means in general, in the absence of either of these four genes, there's less UDP-MurNAc-pentapeptides, causing less AmpR repression, originating less *ampC* repression and therefore higher *ampC* expression, which would lead to an increased resistance to beta-lactams. This is, however, the opposite of what was observed since we observed lower MICs for beta-lactams for all these four mutants.

It is known that the loss of either AmpG or NagZ results in a reduced amount of 1,6-anhMurNAc-peptides and consequently reduced resistance against β -lactam antibiotics, and that the loss of AmpD causes accumulation of 1,6-anhMurNAc-peptides and an increased *ampC* expression. (10,47–49) It is, however, not clear the mechanism through which *anmK*, *mupP*, *amgK* and *murU* impact beta-lactam resistance, increasing it, as well as how they impact *ampC* expression.

One theory is that the reduced resistance is due exclusively to an impact on other resistance mechanisms by unknown means. A possible explanation to such a decrease in beta-lactam resistance in the mutant strains would also be a very accentuated decrease in efflux pump expression, therefore, this was investigated.

The fact that reduced resistance was observed in the deletion mutants of all four gene involved in the PG recycling pathway (*anmK*, *amgK*, *murU* and *mupP*) re-iterates the relevance of the pathway for resistance modulation. The resistance reduction to beta-lactams, fosfomycin and interestingly, polymyxin B, that the mutants exhibit when compared to the WT strain is expressive. This is in accordance with the findings of Sonnabend *et al.*, who concluded that the recycling pathway plays a critical role in resistance against beta-lactam antibiotics, particularly in strains with high beta-lactamase activity. (10)

The *bepA* mutant strain exhibited similar MIC results to the four PG recycling mutants. BepA, previously known as YfgC, is a protease/chaperone for the improvement of the assembly and/ or degradation of β -barrel membrane proteins in the β -barrel assembly machinery (BAM) complex. (46) It is known that the deletion of BAM proteins disturbs outer membrane integrity and increases bacteria's susceptibility to antibiotics. (36,50,51) The fact that BepA directly impacts the BAM complex, which is known to increase the bacteria's susceptibility to antibiotics once one of its proteins is deleted, explains why, when *bepA* is deleted, resistance to antibiotics that specifically interact with the cell wall (such as beta-lactams and polymyxin B) decrease in comparison to the WT strain. In *E. coli*, BepA was shown to be involved in the biogenesis and degradation of LptD. (42) LptD, a beta-barrel protein, is also a component of the LPS translocon and therefore BepA is important for LPS delivery to the outer membrane. (42) Knowing this, in the absence of BepA, one can think it's easier for polymyxin B to interact with the remaining LPS in the OM, thus improving its

action and lowering the necessary minimal inhibitory concentration. This could explain the reduction of resistance observed for the *bepA* deletion mutant to polymyxin B.

3.4. Efflux activity assay

Bacteria have the capacity of transporting potentially toxic compounds, such as antibiotics, out of the cells, through a process denominated efflux. (52) This process is acknowledged as a major cause of intrinsic antibiotic resistance in bacteria, particularly in *Pa* and overexpression of efflux pumps is one of the main resistance mechanisms of MDR *Pa*. (52) Taking this into account, and in order to determine if the increased antibiotic susceptibility of the deletion mutants verified in the MIC assays is due to a reduced activity of efflux pumps, efflux activity assays were performed (Fig. 13).

The efflux activity assay is based on the use of Hoechst 33342, a fluorescent dye, that penetrates the bacterial cell wall and emits blue fluorescence when binding to dsDNA. This dye is a substrate of different efflux pumps, hence, the fluorescence signal reflects the proportion influx and efflux of molecules. High activity of efflux pumps would result in low luminescence levels, as the dye would quickly be removed from the cell.

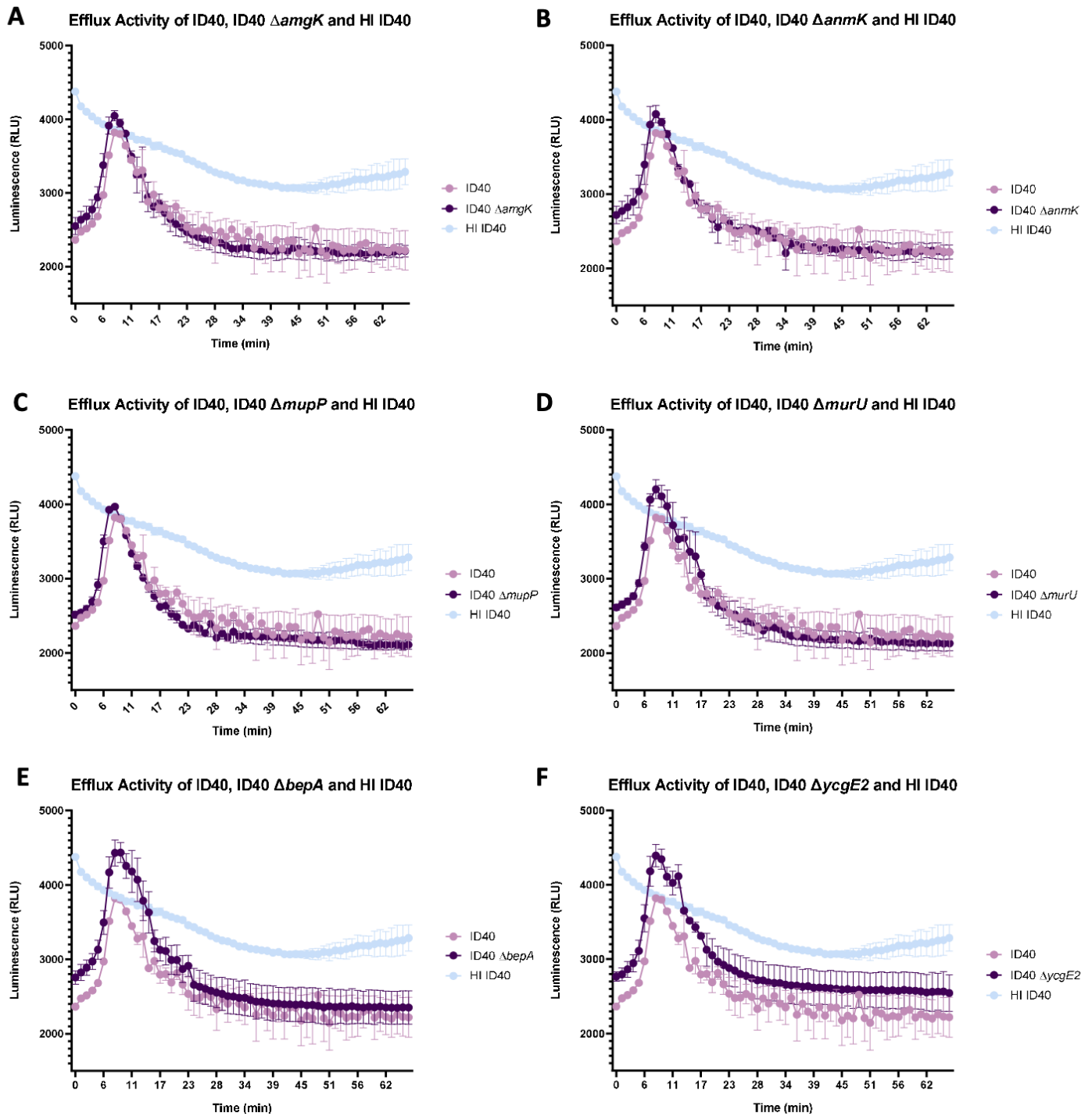


Figure 13 - Efflux activity in ID40 and the deletion mutants ($\Delta amgK$, $\Delta anmK$, $\Delta mupP$, $\Delta murU$, $\Delta bepA$, $\Delta ycgE2$).

The luminescence in relative light units (RLU) of each mutant (dark purple) was compared with the WT ID40 strain (light mauve) and the negative control, HI ID40 (light blue). Luminescence (RLU) was measured every 60 seconds, over a period of 66 minutes. Each curve corresponds to the mean luminescence from 2 replicates, measured at each time-point depicted. The standard error (SEM) of each mean is depicted. HI: Heat inactivated.

After 17 minutes no strain presents higher relative luminescence than the heat inactivated WT, as it shouldn't because this bacterium, being heat inactivated, has absolutely no efflux pump activity. The closest to the relative luminescence of the heat inactivated WT, the lowest the efflux pump activity of the analyzed strain.

The *amgK* mutant strain reveals similar relative luminescence to the WT strain (Figure 13 (A)). Similarly, the *anmK*, *mupP* and *murU* deletion strains exhibit the same relative luminescence as the WT strain (Figure 13 (B, C, D)). These results seem to indicate these mutants have similar efflux pump activity to the WT strain.

On the other hand, in Figure 13 (E) and (F) both the *bepA* and *ycgE2* deletion strains present a slightly higher relative luminescence than the WT strain, however, the size of the error bars does not allow for conclusions to be made.

These results seem to indicate an unaltered efflux pump activity for most, if not all, mutants. As so, the main mechanism responsible for antibiotic resistance that's being affected upon the deletion of each gene is most likely not the efflux pump system.

3.5. Beta-lactamase activity

ID40 has two beta-lactamases encoded: *ampC* and *OXA-486/bla/poxB*. (10) The overproduction of beta-lactamases, like AmpC, which inactivates penicillins, cephalosporins and monobactams, is a common mechanism of resistance. (19)

The mechanism through which *anmK*, *amgK*, *murU*, *mupP*, *bepA* or even *ycgE2* may impact the beta-lactamase AmpC activity is unclear. However, a decrease in antibiotic resistance was clearly observed for all, except *ycgE2*. As so, it is relevant to investigate if any changes occur in beta-lactamase activity.

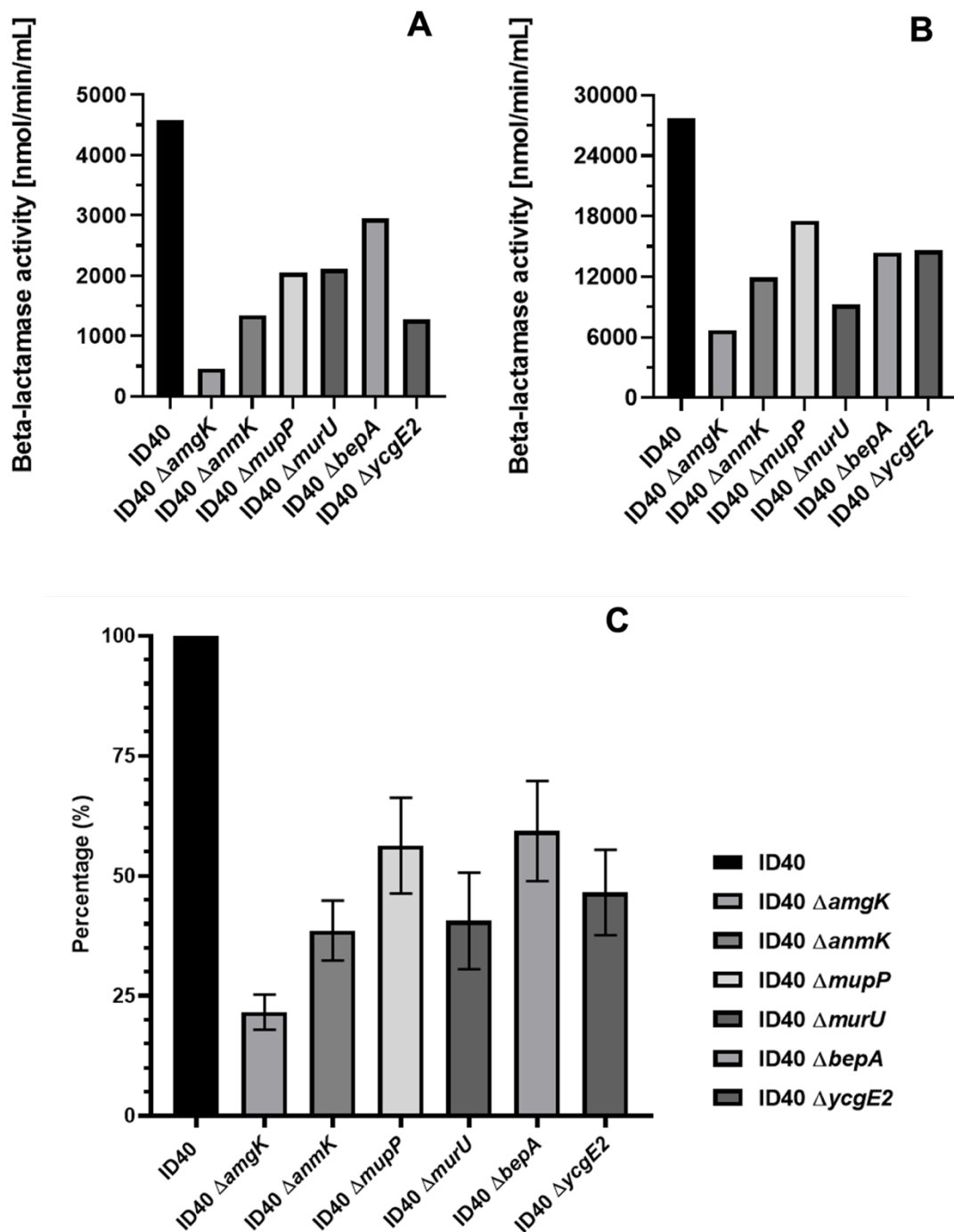


Figure 14 - β -lactamase Activity Assay of ID40 WT and deletion mutants ($\Delta amgK$, $\Delta anmK$, $\Delta mupP$, $\Delta murU$, $\Delta bepA$, $\Delta ycgE2$).

β -lactamase activity is determined by measuring nitrocefin turnover (nmol/min/mL). In (A) and (B) the results from two independent assays are depicted. The mean of the β -lactamase activity from 2 replicates, from the WT and each mutant, for each assay is depicted. In (C) the activity percentages (%) of β -lactamase of both independent experiments are depicted. The standard deviation (sd) of the mean is presented.

In the first set of results, Figure 14 (A), the WT strain beta-lactamase activity is 4500 nmol/min/mL and all the mutant strains present lower activities: 3000 nmol/min/mL for *bepA*, approximately 2000 nmol/min/mL for *mupP* and *murU*, around 1300 nmol/min/mL for *anmK* and *ycgE2* and slightly under 1000 nmol/min/mL for *amgK*.

In the second set, Figure 14 (B), the results vary somewhat, the WT strain beta-lactamase activity is 28000 nmol/min/mL but all the mutants still present lower activities: the lowest being around 7000 nmol/min/mL for *amgK*, followed by 9000 nmol/min/mL for *murU*, 12000 nmol/min/mL for *anmK*, 14500 nmol/min/mL for both *bepA* and *ycgE2* and the highest beta-lactamase activity was recorded for *mupP* at 17500 nmol/min/mL.

From these sets of results, it's clear there's a reduction of beta-lactamase activity for all mutants investigated when compared to the WT strain.

In order to analyze both sets together, percentages were calculated and presented in Figure 14 (C). Once again, all mutants revealed a relevant decrease in beta-lactamase activity. The percentages varied from around 20 % to approximately 60 %, with no mutant exhibiting as much as 60 % of the WT's beta-lactamase activity. More, the *amgK* mutant strain exhibited the lowest percentage of beta-lactamase activity with only around 20 % of the WT strain's activity, which may indicate that the *amgK* gene is indeed of substantial importance for beta-lactamase activity and consequently for resistance modulation. The *anmK* and *murU* mutant strains have the following lowest percentage of beta-lactamase activity at roughly 40 %. The *ycgE2* mutant strain does not have the highest percentage of activity, with its activity of about 45 %, which is not expected based on its MIC assay results. With the highest, but still substantially low, percentages of activity are the *mupP* and *bepA* mutant strains, with around 55 % and 60 % of beta-lactamase activity, respectively.

In ID40, there are two encoded beta-lactamases, *ampC* and *poxB*, however it has been shown that PoxB does not contribute to beta-lactam resistance. (10,13) As so the decreased beta-lactamase activity observed in all mutants must be due to the deleted genes influence on the cephalosporinase AmpC, either on its expression or on its activity, meaning *amgK*, *anmK*, *mupP*, *murU*, *bepA* and *ycgE2* most likely impact beta-lactamase activity and are thus capable of altering the bacteria's susceptibility to beta-lactams. Nonetheless, it is clear that the PG recycling pathway impacts beta-lactamase activity, thus modulating antibiotic resistance.

3.6. mRNA expression

In the ID40 genome both β -lactamases are encoded: *ampC* and *poxB*. For PoxB, it has already been shown that it does not contribute to β -lactam resistance. (10) As so PoxB can't be responsible for the reduction of either antibiotic resistance or beta-lactamase activity and thus looking into its expression is not in the interest of this work. Therefore, we analyzed the gene expression of *ampC* to further investigate which changes in the mutants are responsible for the decreased β -lactamase activity observed.

For analyzing gene expression reverse-transcription quantitative real-time PCR (qRT-PCR) is a widely used method since it provides accurate, sensitive and reproducible results. (53) However, this method sensitivity and specificity can be affected by the presence of residual DNA (gDNA), which is an inherent problem in RNA extraction due to the similar properties of DNA and RNA. (53) Non-specific amplification resulting from gDNA contamination will result in the overestimation of transcript levels. (53) Therefore, a qPCR was done previously to assert minimal presence of gDNA contamination. A housekeeping gene was used for this purpose, *gyrB*, which encodes DNA gyrase subunit B and is stably expressed. (54) The crossing point (CP or CT) is the threshold cycle, meaning the number of cycles required to produce a constant emission of fluorescence. A higher CP value indicates a bigger number of cycles is required to detect the PCR product, thus less exists. Reverse transcriptase is a DNA polymerase enzyme that transcribes RNA into DNA that is then detected, as so, in the presence of the enzyme the CP values should decrease because there should be a PCR product to be detected in earlier cycles.

The resulting CPs from these qPCRs are presented in table 15.

Table 15 - CP value results from qPCRs, with and without the presence of reverse transcriptase. The PCRs were applied to samples of ID40, ID40 Δ *amgK* and H₂O and the *gyrB* set of primers was used. The CP values presented are the mean of quadruplicates.

Without Reverse Transcriptase		With Reverse Transcriptase	
Sample	CP value	Sample	CP value
ID40	32,45	ID40	19,56
Δ <i>amgK</i>	33,25	Δ <i>amgK</i>	19,72
H ₂ O	31,89	H ₂ O	31,89

These results indicate no significant DNA contamination is present.

In light of this, to establish if the beta-lactamase activity observed in the deletion mutants was caused on the transcriptional level, the relative mRNA levels of *ampC* were assessed by qRT-PCR.

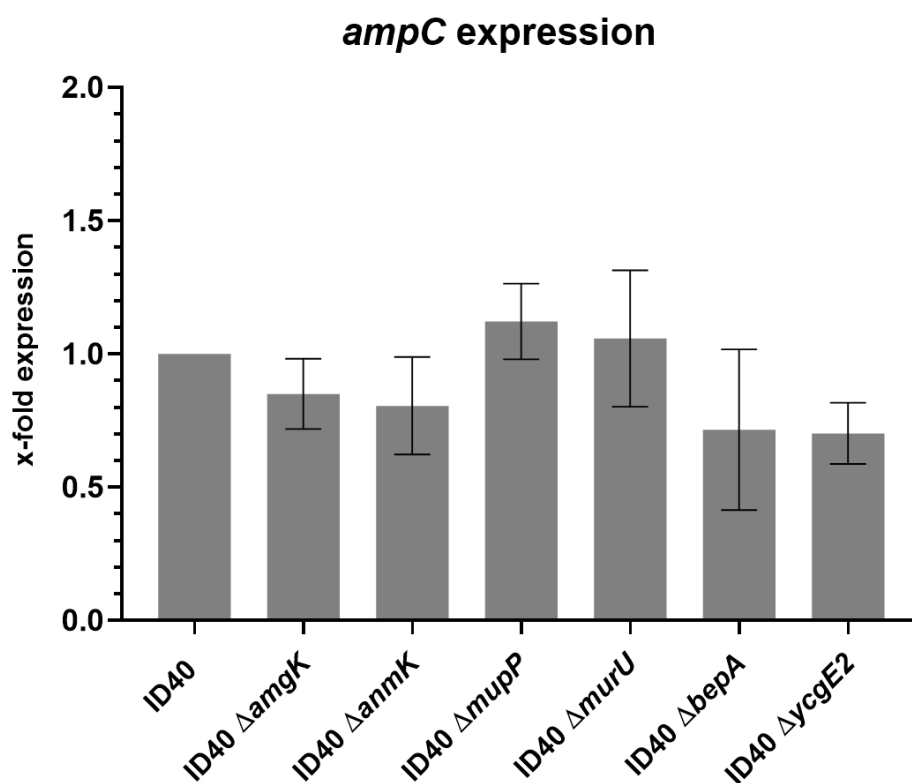


Figure 15 - *ampC* expression in ID40 WT and deletion mutants (Δ amgK, Δ anmK, Δ mupP, Δ murU, Δ bepA, Δ ycgE2).

The expression of the gene *ampC* was determined by qRT-PCR. The mean fold expression of 3 replicates, as well as the corresponding standard deviation were calculated and are presented.

For all mutant strains, the differences in expression are too small, and when taking into consideration the error of the experiment, they become irrelevant as seen in Figure 15. As so, one can conclude that no difference in expression was observed with certainty for neither of the strains analyzed.

Induction of *ampC* expression is mediated by the disruption of PG recycling, as so, it would be expected that some differences would be observed on the expression of *ampC* upon the deletion of genes that directly impact the PG recycling pathway, such as *anmK*, *amgK*, *mupP* and *murU*. Furthermore, the observed decrease in antibiotic resistance and beta-lactamase activity would be expected to result from a decrease in *ampC* expression, which

was not observed. This could suggest that there are unknown factors at play that contribute to the regulation of *ampC* expression.

Moreover, a reduction of *ampC* expression after *amgK* deletion in ID40 has been previously reported by Sonnabend *et al.*, this was not observed in the presented results (Figure 15). (10)

3.7. Serum killing

The complement system constitutes the first line of human immune defense and is made up of a network of plasmatic proteins that trigger a proteolytic cascade upon recognition of certain microbial patterns. (40,41) With that said, bacteria are able to use several and very intricate strategies to control, modulate and block the host's complement system. (41) For instance, changes in LPS can lead to changes in complement resistance. (40)

Results from the MIC assay for polymyxin B showed that deletion of either *amgK* or *bepA* resulted in a 2-fold reduction of the MIC value (from a MIC of 4 µg/mL to 1 µg/mL). This led to the idea that these genes might act on the LPS structure. Since the LPS structure is highly important to achieve serum resistance it was speculated that deletion of *amgK* or *bepA* might affect serum resistance. Due to time restrictions, we focused on the *amgK* gene.

The serum killing assay performed is a luminescence-based method to detect surviving bacteria by measuring their ATP. (36,55) The measured luminescence signal, interpreted as luciferase activity, is proportional to the ATP present, which is in turn directly proportional to the number of viable bacteria. (55)

In this assay *P. aeruginosa* strains and their corresponding *amgK* deletion mutants are incubated with different concentrations of normal human serum (NHS) and heat inactivated serum (HIS) and the luminescence is then measured, allowing to compare the survival of the tested strains.

As so, by observing whether serum resistance of Pa is altered in the *amgK* mutant the serum killing assay may provide data to further characterize the *amgK* gene.

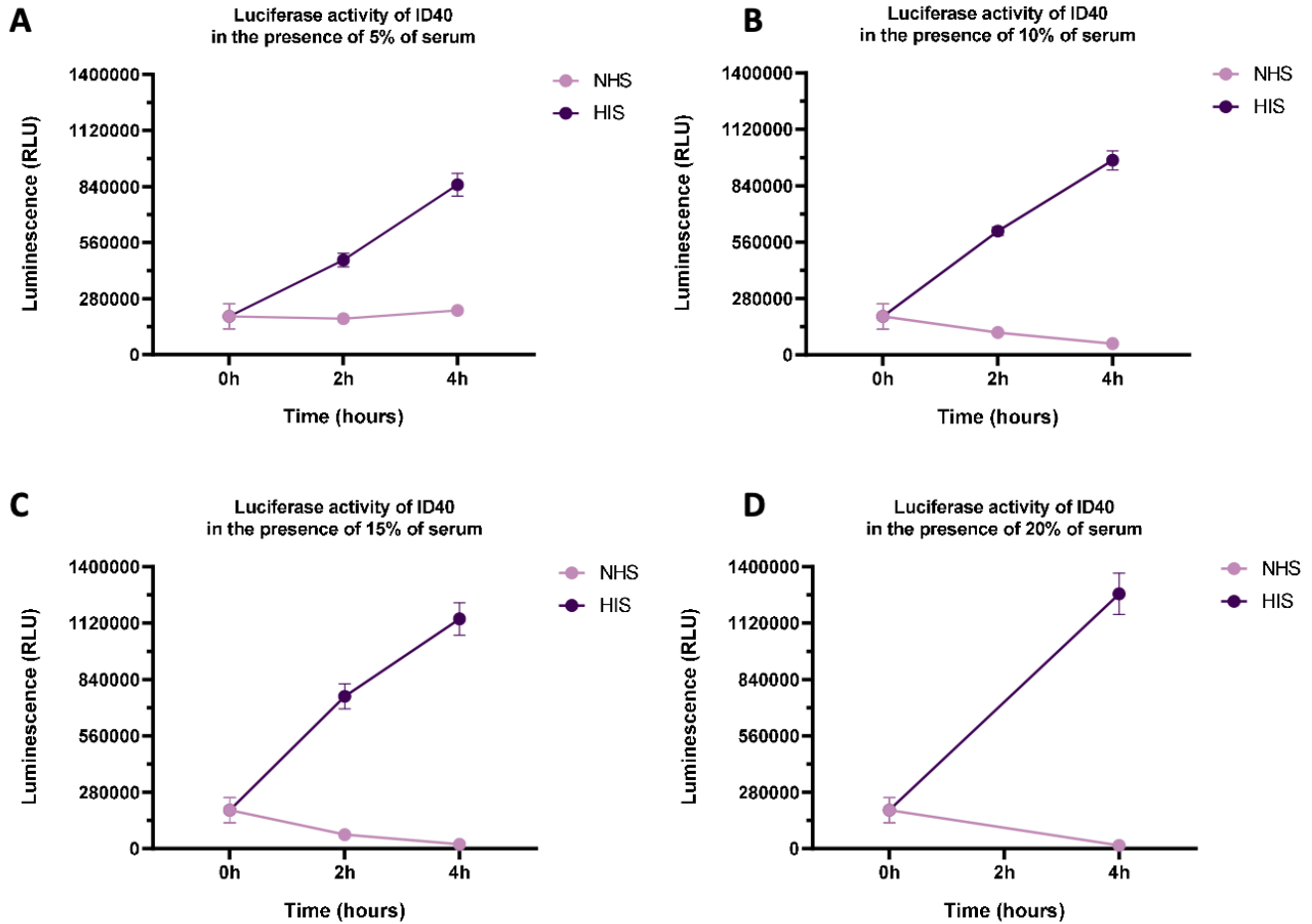


Figure 16 - Serum killing assay for assessment of optimal human serum concentration for ID40 WT strain. Survival of ID40 WT strain was assessed by measuring luminescence (RLU) at 0, 2, and 4 hours of incubation in (A) 5 %, (B) 10 %, (C) 15 % and (D) 20 % of inactivated human serum (dark purple) and normal human serum (light mauve). All assays were performed at 37°C. Data are shown as mean \pm standard deviation (sd). NHS: Normal human serum; HIS: Heat inactivated human serum.

Because ID40 is a clinical isolate strain it is more sensitive to normal human serum, as so, at concentrations as low as 5 % to 10 % the WT strain is already dying, thus rendering assays at these concentrations not relevant for comparing the WT with a mutant strain. (Fig. 16) For this reason PAO1 and PA14 were used instead to investigate whether *amgK* contributes to serum resistance.

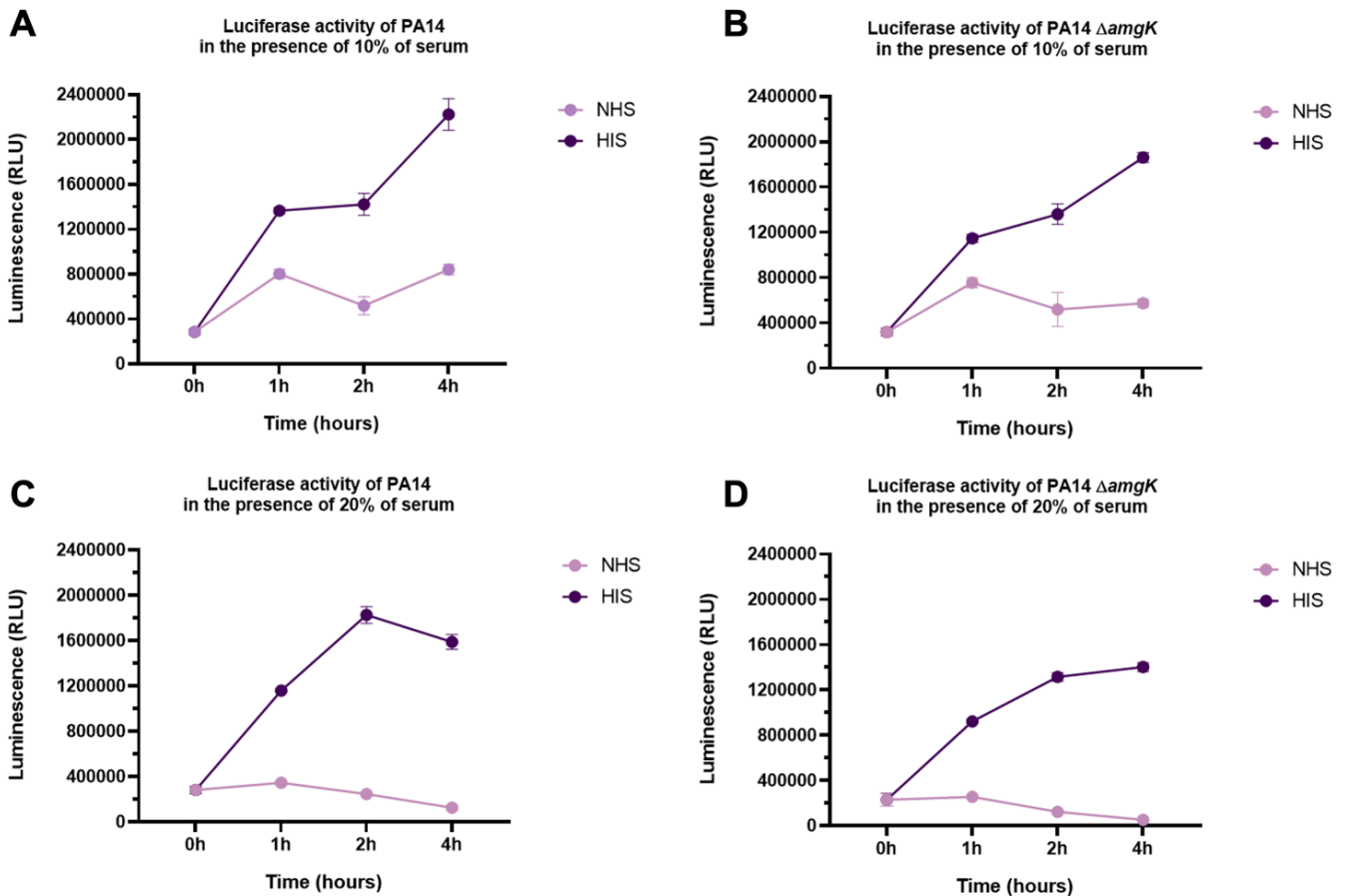


Figure 17 - Serum killing assay of PA14 *P. aeruginosa* strain and the PA14 $\Delta amgK$ mutant.

Survival of each strain was assessed by measuring luminescence (RLU) at 0, 1, 2, and 4 hours of incubation of: PA14 (WT and *amgK* mutant) in (A) 10 % and (B) 20 % of human sera. All assays were performed at 37°C. The results of each strain exposed to NHS (light mauve) and to HIS (dark purple) are depicted. NHS: Normal human serum; HIS: Heat inactivated human serum.

Upon observation of the PA14 strain with 10 % human serum (Figure 17 (A)) one can infer that, in the WT strain, the cells start dying in the presence of normal human serum (NHS) from 1 to 2 hours but are able to resist it and from 2 to 4 hours are able to grow. In the presence of heat inactivated serum (HIS) the cells seem to stop growing from 1 to 2 hours, without dying, and grow more rapidly than in the presence of NHS, from 2 to 4 hours. When looking

at the PA14 *amgK* deletion mutant (Figure 17 (B)), the same general behaviour, which is similar to the WT strain, is observed for both NHS and HIS.

In the presence of 20 % normal human serum both the PA14 WT and the PA14 $\Delta amgK$ (Figure 17 (C) and (D)) exhibit a constant decrease in luminescence from 1 hour forward, thus the cells die. With 20 % HIS, the cells seem to survive in both the WT and *amgK* mutant strain. This may mean the 20 % concentration of serum may be too high to compare the WT strain with a mutant deletion strain, resulting in the rapid death of both strains.

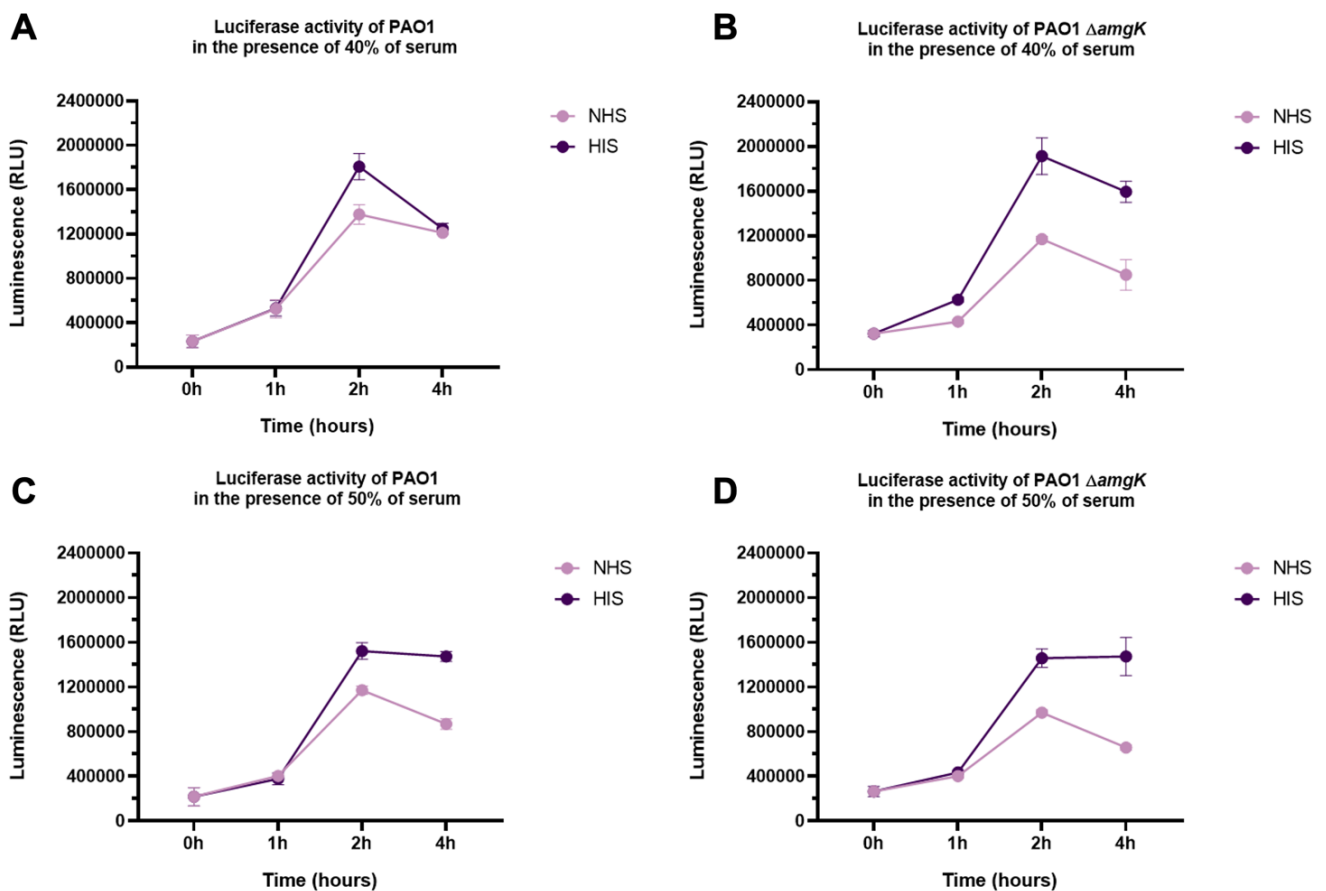


Figure 18 - Serum killing assay of PAO1 *P. aeruginosa* strain and the PAO1 $\Delta amgK$ mutant.

Survival of each strain was assessed by measuring luminescence (RLU) at 0, 1, 2, and 4 hours of incubation of: PAO1 (WT and *amgK* deletion mutant) in (A) 40 % and (B) 50 % of human sera. All assays were performed at 37°C. The results of each strain exposed to NHS (light mauve) and to HIS (dark purple) are depicted. NHS: Normal human serum; HIS: Heat inactivated human serum.

In the PAO1 strain, when using 40 % human serum, the *amgK* mutant strain (Figure 18 (B)) seems to have a harder time growing in the presence of NHS from 0 to 1 hour exhibiting a smaller increase in luminescence than the WT strain (Figure 18 (A)), then recuperates from 1

to 2 hours but still exhibiting a lesser increase in luminescence than the WT strain (Figure 18 (A) and (B)). From 2 to 4 hours, in the same conditions, the *amgK* deletion mutant cells show a decrease in ATP production while the WT cells only show a slight decrease (Figure 18 (A) and (B)), this difference however doesn't seem significant enough to allow for any conclusions. A parallel behaviour between both strains is observed when 40 % of the HIS is used, until 2 hours. After the 2-hour time point, even though both strains present a decrease in luminescence, surprisingly, the WT strain's luminescence has a bigger decline (Figure 18 (A) and (B)). This seems to be an artifact and have no significance, firstly because the behaviour is not seen in the curve made in the presence of NHS but only on the HIS, which is not logical, and secondly because it's also not seen on the 50 % HIS assay (Figure 18 (C) and (D)).

When using 50 % of human serum in PAO1, using either HIS or NHS resulted in a similar response in the WT strain (Figure 18 (C)), meaning cells were alive and therefore resisting the complement system, only after 2 hours of incubation with NHS, did the luminescence start to diminish. A similar behaviour was observed in the *amgK* mutant (Figure 18 (D)).

The deletion of *amgK* seemed to have insignificant impact on survival in the presence of normal human serum, and thus insignificant impact on serum complement system resistance. Since no significant difference was observed, there seems to be no robust difference in serum resistance between the WT strain and the *amgK* mutant strain.

It would, perhaps, had been more advantageous to investigate the serum resistance of the *bepA* mutant which we were unable to do, due to time constraints. Since BepA contributes to the maintenance of outer membrane structural and functional integrity, it is expected that the deletion of *bepA* would result in decreased resistance to the human complement system. If this is confirmed, it would exacerbate the interest of *bepA* as a target of further studies for antibiotic resistance.

4. Conclusion

Overall, the main goal of this thesis was achieved as we were able to understand that the genes *anmK*, *mupP*, *murU*, *amgK* and *bepA* lead to increased beta-lactam resistance, thus constituting possible antibiotic targets. A relevant increase in resistance to polymyxin B was ascertained for *amgK* and *bepA*. Additionally, an increased resistance to fosfomycin was also observed for all genes, including *ycgE2*.

The resistance increase caused by either *anmK*, *mupP*, *murU* or *amgK*, all involved in the salvage/recycling pathway, suggest the pathway plays a critical role in peptidoglycan recycling and modulates antibiotic resistance. All genes of this pathway seem to be critical for antibiotic resistance. It was also concluded that the general fitness of the bacteria is not affected by *anmK*, *mupP*, *murU* or *amgK*, meaning the recycling pathway doesn't seem to influence bacterial fitness under normal conditions. No obvious impact on efflux/influx was observed for these genes either. Even though *anmK*, *mupP*, *murU* or *amgK* individually contribute to beta-lactamase activity, surprisingly, the *ampC* expression was not affected when the genes were individually deleted. As so, how these genes are involved in transcriptional regulation of the β -lactamase AmpC and the mechanism through which they modulate resistance remains unclear. Further, *amgK* doesn't seem to increase resistance to the human complement system.

bepA, like the genes involved in the PG recycling pathway, showed no influence in bacterial fitness, and also contributed to an increase in beta-lactamase activity, which explains the increased beta-lactam resistance observed for this gene even when the *ampC* expression was not affected like with the recycling pathway mutants. The most likely mechanism of resistance to beta-lactams that *bepA* participates in is involving the outer membrane maintenance, as evidenced for instance by the polymyxin B results, and remains unclear. A serum killing assay with a *bepA* deletion mutant would be significant in helping to clarify this.

The gene *ycgE2* doesn't seem to impact antibiotic resistance but interestingly, its deletion mutant exhibited a decrease in beta-lactamase activity suggesting the gene leads to increased beta-lactamase activity. *ycgE2* also showed no impact in bacterial fitness as well as in

efflux/influx, and no significant difference in *ampC* expression. As so, its role in beta-lactam resistance could not be validated.

In the future, the serum killing assay with the *bepA* deletion mutant would definitely be a priority, in order to understand if *bepA*'s involvement in outer membrane maintenance is relevant in the resistance modulation. It would also be very important to further validate the *ampC* expression results, by for instance, repeating the assay, including more controls such as expression of the deleted genes.

5. References

1. Cabot G, Ocampo-Sosa AA, Tubau F, Macia MD, Rodríguez C, Moya B, et al. Overexpression of AmpC and efflux pumps in *Pseudomonas aeruginosa* isolates from bloodstream infections: Prevalence and impact on resistance in a Spanish multicenter study. *Antimicrob Agents Chemother*. 2011;55(5):1906–11.
2. Wu W, Jin Y, Bai F, Jin S. *Pseudomonas aeruginosa*. In: *Molecular Medical Microbiology*. Elsevier; 2014. p. 753–67.
3. Tsang KW, Ng P, Ho PL, Chan S, Tipoe G, Leung R, et al. Effects of erythromycin on *Pseudomonas aeruginosa* adherence to collagen and morphology *in vitro*. *European Respiratory Journal*. 2003 Mar;21(3):401–6.
4. Caldwell CC, Chen Y, Goetzmann HS, Hao Y, Borchers MT, Hassett DJ, et al. *Pseudomonas aeruginosa* Exotoxin Pyocyanin Causes Cystic Fibrosis Airway Pathogenesis. *Am J Pathol*. 2009 Dec;175(6):2473–88.
5. Pang Z, Raudonis R, Glick BR, Lin TJ, Cheng Z. Antibiotic resistance in *Pseudomonas aeruginosa*: mechanisms and alternative therapeutic strategies. Vol. 37, *Biotechnology Advances*. Elsevier Inc.; 2019. p. 177–92.
6. Gisin J, Schneider A, Nägele B, Borisova M, Mayer C. A cell wall recycling shortcut that bypasses peptidoglycan de novo biosynthesis. *Nat Chem Biol*. 2013 Aug;9(8):491–3.
7. May KL, Grabowicz M. The bacterial outer membrane is an evolving antibiotic barrier. *Proceedings of the National Academy of Sciences*. 2018 Sep 4;115(36):8852–4.
8. Sharma AK, Dhasmana N, Dubey N, Kumar N, Gangwal A, Gupta M, et al. Bacterial Virulence Factors: Secreted for Survival. *Indian J Microbiol*. 2017 Mar 5;57(1):1–10.
9. Bassetti M, Vena A, Croxatto A, Righi E, Guery B. How to manage *Pseudomonas aeruginosa* infections. Vol. 7, *Drugs in Context*. Bioexcel Publishing LTD; 2018.
10. Sonnabend MS, Klein K, Beier S, Angelov A, Kluj R, Mayer C, et al. Identification of drug resistance determinants in a clinical isolate of *Pseudomonas aeruginosa* by high-density transposon mutagenesis. *Antimicrob Agents Chemother*. 2020;64(3).
11. Tacconelli E, Carrara E, Savoldi A, Kattula D, Burkert F. GLOBAL PRIORITY LIST OF ANTIBIOTIC-RESISTANT BACTERIA TO GUIDE RESEARCH, DISCOVERY, AND

- DEVELOPMENT OF NEW ANTIBIOTICS [Internet]. 2017. Available from: <http://www.cdc.gov/drugresistance/threat-report-2013/>
12. Tacconelli E, Carrara E, Savoldi A, Harbarth S, Mendelson M, Monnet DL, et al. Discovery, research, and development of new antibiotics: the WHO priority list of antibiotic-resistant bacteria and tuberculosis. *Lancet Infect Dis*. 2018 Mar;18(3):318–27.
 13. Dhar S, Kumari H, Balasubramanian D, Mathee K. Cell-wall recycling and synthesis in *Escherichia coli* and *Pseudomonas aeruginosa* – Their role in the development of resistance. Vol. 67, *Journal of Medical Microbiology*. Microbiology Society; 2018. p. 1–21.
 14. Potron A, Poirel L, Nordmann P. Emerging broad-spectrum resistance in *Pseudomonas aeruginosa* and *Acinetobacter baumannii*: Mechanisms and epidemiology. Vol. 45, *International Journal of Antimicrobial Agents*. Elsevier B.V.; 2015. p. 568–85.
 15. Borisova M, Gisin J, Mayer C. Blocking peptidoglycan recycling in *Pseudomonas aeruginosa* attenuates intrinsic resistance to fosfomycin. In: *Microbial Drug Resistance*. Mary Ann Liebert Inc.; 2014. p. 231–7.
 16. Barquist L, Mayho M, Cummins C, Cain AK, Boinett CJ, Page AJ, et al. The TraDIS toolkit: Sequencing and analysis for dense transposon mutant libraries. *Bioinformatics*. 2016 Apr 1;32(7):1109–11.
 17. Jana B, Cain AK, Doerrler WT, Boinett CJ, Fookes MC, Parkhill J, et al. The secondary resistome of multidrug-resistant *Klebsiella pneumoniae*. *Sci Rep*. 2017 Feb 15;7.
 18. Borisova M, Gisin J, Mayer C. The N-acetylmuramic acid 6-phosphate phosphatase MupP completes the *pseudomonas* peptidoglycan recycling pathway leading to intrinsic fosfomycin resistance. *mBio*. 2017 Mar 1;8(2).
 19. Fumeaux C, Bernhardt TG. Identification of MupP as a New Peptidoglycan Recycling Factor and Antibiotic Resistance Determinant in *Pseudomonas aeruginosa*. 2017; Available from: <https://doi.org/10.1128/mBio.00092-17>.
 20. Buhl M, Kästle C, Geyer A, Autenrieth IB, Peter S, Willmann M. Molecular Evolution of Extensively Drug-Resistant (XDR) *Pseudomonas aeruginosa* Strains From Patients and Hospital Environment in a Prolonged Outbreak. *Front Microbiol*. 2019 Aug 8;10.

21. Hmelo LR, Borlee BR, Almblad H, Love ME, Randall TE, Tseng BS, et al. Precision-engineering the *Pseudomonas aeruginosa* genome with two-step allelic exchange. *Nat Protoc.* 2015 Oct 22;10(11):1820–41.
22. Lehman MK, Bose JL, Bayles KW. Allelic Exchange. In 2014. p. 89–96.
23. Gibson DG, Young L, Chuang RY, Venter JC, Hutchison CA, Smith HO. Enzymatic assembly of DNA molecules up to several hundred kilobases. *Nat Methods.* 2009;6(5):343–5.
24. Griffiths AJ, Lewontin William M, Gelbart David T, Suzuki RC. *An Introduction to Genetic Analysis* Eighth Edition. 2004.
25. Frost LS. Conjugation, Bacterial. In: *Encyclopedia of Microbiology.* Elsevier; 2009. p. 517–31.
26. Komorniczak M. File:Bacterial growth en.svg. https://commons.wikimedia.org/wiki/File:Bacterial_growth_en.svg. 2009.
27. Myers JA, Curtis BS, Curtis WR. Improving accuracy of cell and chromophore concentration measurements using optical density. *BMC Biophys.* 2013 Dec 22;6(1):4.
28. Andrews JM. Determination of minimum inhibitory concentrations. *Journal of Antimicrobial Chemotherapy.* 2001 Jul 1;48(suppl_1):5–16.
29. Puzari M, Chetia P. RND efflux pump mediated antibiotic resistance in Gram-negative bacteria *Escherichia coli* and *Pseudomonas aeruginosa*: a major issue worldwide. *World J Microbiol Biotechnol.* 2017 Feb 2;33(2):24.
30. Coldham NG, Webber M, Woodward MJ, Piddock LJ v. A 96-well plate fluorescence assay for assessment of cellular permeability and active efflux in *Salmonella enterica* serovar Typhimurium and *Escherichia coli*. *Journal of Antimicrobial Chemotherapy.* 2010 Aug 1;65(8):1655–63.
31. van den Berg van Saparoea HB, Lubelski J, van Merkerk R, Mazurkiewicz PS, Driessen AJM. Proton Motive Force-Dependent Hoechst 33342 Transport by the ABC Transporter LmrA of *Lactococcus lactis*. *Biochemistry.* 2005 Dec 1;44(51):16931–8.
32. Siriyong T, Srimanote P, Chusri S, Yingyongnarongkul B ek, Suaisom C, Tipmanee V, et al. Conessine as a novel inhibitor of multidrug efflux pump systems in *Pseudomonas aeruginosa*. *BMC Complement Altern Med.* 2017 Dec 14;17(1):405.

33. Kong KF, Schneper L, Mathee K. Beta-lactam antibiotics: From antibiosis to resistance and bacteriology. Vol. 118, APMIS. 2010. p. 1–36.
34. Bulychev A, Mobashery S. Class C-Lactamases Operate at the Diffusion Limit for Turnover of Their Preferred Cephalosporin Substrates. Vol. 43, ANTIMICROBIAL AGENTS AND CHEMOTHERAPY. 1999.
35. Gudnason H, Dufva M, Bang DD, Wolff A. Comparison of multiple DNA dyes for real-time PCR: effects of dye concentration and sequence composition on DNA amplification and melting temperature. Nucleic Acids Res. 2007 Oct;35(19):e127.
36. Klein K, Sonnabend MS, Frank L, Leibiger K, Franz-Wachtel M, Macek B, et al. Deprivation of the Periplasmic Chaperone SurA Reduces Virulence and Restores Antibiotic Susceptibility of Multidrug-Resistant *Pseudomonas aeruginosa*. Front Microbiol. 2019;10(FEB).
37. Pfaffl MW. A new mathematical model for relative quantification in real-time RT-PCR. Vol. 29, Nucleic Acids Research. 2001.
38. Silver N, Best S, Jiang J, Thein SL. Selection of housekeeping genes for gene expression studies in human reticulocytes using real-time PCR. BMC Mol Biol. 2006 Dec 6;7(1):33.
39. Larionov A, Krause A, Miller W. A standard curve based method for relative real time PCR data processing. BMC Bioinformatics. 2005;6(1):62.
40. Doorduyn DJ, Rooijackers SHM, van Schaik W, Bardoel BW. Complement resistance mechanisms of *Klebsiella pneumoniae*. Immunobiology. 2016 Oct;221(10):1102–9.
41. Zipfel PF, Hallström T, Riesbeck K. Human complement control and complement evasion by pathogenic microbes – Tipping the balance. Mol Immunol. 2013 Dec;56(3):152–60.
42. Miyazaki R, Watanabe T, Yoshitani K, Akiyama Y. Edge-strand of BepA interacts with immature LptD on the β -barrel assembly machine to direct it to on- and off-pathways. Elife. 2021 Aug 31;10.
43. Barnes WM. PCR amplification of up to 35-kb DNA with high fidelity and high yield from lambda bacteriophage templates. Proceedings of the National Academy of Sciences. 1994 Mar 15;91(6):2216–20.
44. BioLabs Inc NE. Gibson Assembly Master Mix E2611 manual Gibson Assembly Cloning Kit E5510 manual [Internet]. Available from: <http://www.neb.com/TmCalculator>.

45. Park JT, Uehara T. How Bacteria Consume Their Own Exoskeletons (Turnover and Recycling of Cell Wall Peptidoglycan). *Microbiology and Molecular Biology Reviews*. 2008 Jun;72(2):211–27.
46. Shahrizal M, Daimon Y, Tanaka Y, Hayashi Y, Nakayama S, Iwaki S, et al. Structural Basis for the Function of the β -Barrel Assembly-Enhancing Protease BepA. *J Mol Biol*. 2019 Feb 1;431(3):625–35.
47. Jacobs C, Joris B, Jamin M, Klarsov K, Beeumen J, Mengin-Lecreux D, et al. AmpD, essential for both beta-lactamase regulation and cell wall recycling, is a novel cytosolic N-acetylmuramyl-L-alanine amidase. *Mol Microbiol*. 1995 Feb;15(3):553–9.
48. Stubbs KA, Scaffidi A, Debowski AW, Mark BL, Stick R v., Vocadlo DJ. Synthesis and use of mechanism-based protein-profiling probes for retaining β -D-glucosaminidases facilitate identification of *Pseudomonas aeruginosa* NagZ. *J Am Chem Soc*. 2008 Jan 9;130(1):327–35.
49. Lamers RP, Nguyen UT, Nguyen Y, Buensuceso RNC, Burrows LL. Loss of membrane-bound lytic transglycosylases increases outer membrane permeability and β -lactam sensitivity in *Pseudomonas aeruginosa*. *Microbiologyopen*. 2015 Dec 1;4(6):879–95.
50. Weirich J, Bräutigam C, Mühlenkamp M, Franz-Wachtel M, Macek B, Meuskens I, et al. Identifying components required for OMP biogenesis as novel targets for antiinfective drugs. *Virulence*. 2017 Oct 3;8(7):1170–88.
51. Lee KM, Lee K, Go J, Park IH, Shin JS, Choi JY, et al. A Genetic Screen Reveals Novel Targets to Render *Pseudomonas aeruginosa* Sensitive to Lysozyme and Cell Wall-Targeting Antibiotics. *Front Cell Infect Microbiol*. 2017 Mar 1;7.
52. Ryan BM, Dougherty TJ, Beaulieu D, Chuang J, Dougherty BA, Barrett JF. Efflux in bacteria: what do we really know about it? *Expert Opin Investig Drugs*. 2001 Aug 24;10(8):1409–22.
53. Hashemipetroudi SH, Nematzadeh G, Ahmadian G, Yamchi A, Kuhlmann M. Assessment of DNA Contamination in RNA Samples Based on Ribosomal DNA. *Journal of Visualized Experiments*. 2018 Jan 22;(131).
54. Yamamoto S, Harayama S. PCR amplification and direct sequencing of *gyrB* genes with universal primers and their application to the detection and taxonomic analysis of *Pseudomonas putida* strains. *Appl Environ Microbiol*. 1995 Mar;61(3):1104–9.

55. Necchi F, Saul A, Rondini S. Development of a high-throughput method to evaluate serum bactericidal activity using bacterial ATP measurement as survival readout. *PLoS One*. 2017 Feb 13;12(2):e0172163.